Streamlining Tissue Engineering Workflows: Comparing Tissue Formation Between Freshly Cultured and Directly Thawed Cells

A Thesis

Submitted to the Faculty of the

WORCESTER POLYTECHNIC INSTITUTE

In partial fulfillment of the requirements for the

Degree of Master of Science
In Biomedical Engineering

April 2023

By

_____

Timothy Santos-Heiman

Approved

_____

Catherine F. Whittington, Ph.D.
Assistant Professor
Department of Biomedical Engineering
Worcester Polytechnic Institute
Committee Chair

_____

Kristen L. Billiar, Ph.D.
Professor and Department Head
Department of Biomedical Engineering
Worcester Polytechnic Institute
Committee Member

_____

Marsha W. Rolle, Ph.D.
Professor
Department of Biomedical Engineering
Worcester Polytechnic Institute
Thesis Advisor

Table of Contents

Table of Figures

Table of Tables

Acknowledgements

I want to thank everyone who has helped me out along the way through my time in undergrad at WPI all the way through to the completion of my thesis.

I want to thank my advisor Dr. Marsha Rolle for the support, guidance and kindness she has shown me throughout my time working in her lab.

I would like to thank my committee members Dr. Catherine Whittington and Dr. Kristen Billiar for their support, feedback, and guidance throughout my thesis.

Thank you to everyone in Rolle lab. I would like to thank Andre Figueroa Milla for all his help and kindness during my time here, and for his knack for creating mechanical testing gear. I want to thank Will DeMaria for his help and feedback.

Finally, I would also like to thank Jyotsna Patel for her help and training of histology during this project, and Chris Bellerive for guidance and access to the NC-200 at the WPI Biomanufacturing Education and Training Center.

Abstract

Expansion of cells, a fundamental component of engineered tissues, requires lengthy culture and planning times that impede the development of readily available tissue engineered products. One way to improve the overall tissue engineering workflow may be the production and use of pre-made frozen cell stocks that can be used directly without the need for additional culture or recovery time. This thesis analyzes the ability of freshly thawed (FT) rat aortic smooth muscle cells to form scaffold-free tissue rings and compares the stability, metabolic activity, structural and mechanical properties to tissues formed from cells that have been cultured for several days prior to tissue development (normally cultured; NC). Although we observed a statistically significant reduction in cell viability in FT cells compared to NC control cells prior to cell seeding and tissue development, we did not observe significant differences in tissue ring formation, structure, metabolic activity, or mechanical properties. The ability for tissues to be formed on-demand from a premade cell stock allows for the decoupling of cell expansion from the tissue engineering workflow, allowing for more rapid production of tissue engineered constructs, and the potential for lowered operating costs and time delays associated with tissue manufacturing.

Chapter 1: Introduction and Project Aims

In the 37 years since its formal inception, the tissue engineering field has brought humanity a wealth of knowledge regarding human physiology and has helped to create a number of breakthrough medical treatments that would not have been possible without the field. Such examples include Integra, an acellular scaffold used to repair and re-functionalize skin in burn wounds, which is now considered a standard of care, or osteomesh, a widely used product that aids in the regeneration of craniofacial bone.[1-2] The importance of advancements in tissue repair or replacement and disease modeling is fueled by the desire to improve the length and quality of human life. There are many clinical issues inhibiting this effort, with very few having a satisfactory solution. Two of the largest clinical issues are the existence and emergence of diseases without any type of drug or treatment, as well as the abundance of patients awaiting organ transplantation. The current process for researching untreated diseases is incredibly inefficient, with the NIH estimating that around 80-90% of pharmaceutical candidates fail before even reaching clinical testing. This inefficiency in preclinical testing leads to steep increases in research and development costs, with some estimates predicting the cost of development doubling every 9 years.[3] Additionally. The lack of a suitable supply or alternative to donor organ transplantation contributes to excess mortality, with one study finding that 10 people died every day awaiting kidneys between 2008-2015.[4] The development and advancement in tissue engineering processes possesses may address both of these issues by ultimately creating artificial tissue capable of mimicking human physiology for use as more accurate disease models, or artificial organs to be used in lieu of a donor organ.

As field of tissue engineering is incredibly broad, it is difficult for a simple definition to fully encapsulate its entirety, however, it is generally regarded as "An interdisciplinary science involving the use of biological sciences and engineering to develop tissues that restore, maintain, or enhance tissue function.[5]" One of the core concepts of tissue engineering is the triad of three key components that make up engineered tissues: biomaterials, signaling/conditioning, and cells.[5] Cells are the core raw material, needed in virtually every tissue engineering application. The use of mammalian cells allows for the recreation or mimicry of native tissue physiology but requires large quantities of cells to be prepared and produced, often numbering in the hundreds of millions to billions of cells.[6] Traditional 2D cell expansion methods involve lengthy culture

times, which must be factored into experimental workflows and represent an inefficiency in tissue manufacturing. The expansion process takes upwards of 2-3 days to a week depending on doubling time, and in facilities designed specifically for cell expansion, maintenance costs alone can reach upwards of $2.2 million/year.[7-8] Thus, there exists the opportunity for process improvement by decoupling the processes of cell culture and tissue manufacturing, which can be done through the creation and utilization of a pre-made frozen cell bank, with cells ready to use immediately upon thaw (freshly thawed; FT).

It is already common practice for cells to be frozen and banked as part of both contingency planning should any unwanted contamination or differentiation of cells occur in culture, and for storage and shipment of a variety of cell types.[9] The use of a frozen cell bank allows for a large allotment of cells to be grown up in advance to allow for a large bank of materials for scientists to use or purchase for experimentation. The decoupling of these two processes not only allows for more streamlined workflows, but also decreases batch to batch variability through a mass expansion of cells at once under the same conditions. Additionally, it allows for the industrial manufacturing of cells that can be bought and directly used in tissue engineering, without the need for post-thaw plating, expansion, trypsinization and recovery. However, cryopreserving cells has been shown to cause both immediate and delayed damage to the cells[10]. Thus, this thesis project evaluated the feasibility of using freshly thawed (FT) cells from a pre-made cell stock for the creation of scaffold-free engineered vascular tissue derived entirely of cells, when compared to normally cultured (NC) cells used for the same purpose. To this end a tissue ring model, devised in the Rolle lab, composed solely of rat aortic smooth muscle cells (RASMCs) will be used for testing.[11-20] The model provides a high throughput, scaffold free tissue model with low sample-sample variability for structural and functional testing.

This project is comprised of two research aims with distinct hypotheses:

Aim 1. **Evaluate cell viability, tissue ring formation and stability, and metabolic activity of engineered tissue rings**. The tissue rings will be comprised of freshly thawed (FT) rat aortic smooth muscle cells (RASMCs) compared to tissue rings comprised of control cells that were expanded and trypsinized prior to tissue ring formation (“normal culture”; NC). We hypothesize that prior to cell seeding to form tissue rings, NC cells will have higher viability than FT cells due to the storage of FT cells in cytotoxic cryoprotective agents.[9] However, we also

hypothesize that there will be no statistically significant difference in ring formation, stability or metabolic activity between the NC and FT tissue ring groups.

Aim 2. **Evaluate structural properties of tissue rings including thickness, tissue ring morphology, and mechanical integrity of NC and FT tissue rings**. We hypothesize that there will be no structural or mechanical differences between the NC and FT tissue ring groups.

Chapter 2: Background and Literature Review

2.1 Tissue Engineering

Tissue engineering as a recognized scientific field is relatively new, with its modern recognition and definition only being established by the National Science Foundation in 1988.[21] Although great progress has been achieved, issues such as the inability to provide sufficient artificial angiogenesis for nutrient transport or the identification of the optimal biomaterials for synthetic tissue.[5,22]

Despite these drawbacks and limitations, the potential of tissue engineering to revolutionize the medical and pharmaceutical fields is profound. The successful modeling of various tissues and disease states in the human body would allow for faster, and more accurate in vitro testing prior to clinical trials.[23] Current pre-clinical testing relies heavily on outdated and inefficient models. One of the most common models used are animals, which have distinct species-species differences and ethical concerns for their use in testing. Another currently used method is 2D cell-based drug screening assays to test for initial adverse effects of formulated treatments.[24] However, both models do not properly recapitulate human physiology. [25] The lack of clinically translatable models has led to an abundance of resources being placed into research of treatments that appear promising in these models, only to fail once undergoing clinical trials. The cost of developing a new drug has been estimated at around $2.6 billion, with only 0.1% of drug candidates translating from preclinical studies into human testing.[26] Currently there is a decline in the number of FDA approved drugs, and it is estimated that only around 10% of all drugs that enter phase 1 clinical trials will gain FDA approval.[24] The ability to mimic disease states and replicate human physiology allows for the improvements to current drug testing methods, providing more accurate initial data, and an enhanced pathway to market. The other area where tissue engineering can improve the medical field is the repair and replacement of injured and diseased tissue. Tissue engineering's role can vary in this regard, ranging from being a transport vehicle for cellular based therapies, to a means of manufacturing artificial organs.[21]

Tissue engineering can be more easily conceptualized by what is known as the tissue engineering triad, a concept outlining the three key components utilized and required for the development of engineered tissues: cells, biomaterials, and signals.[27] Cells represent the core raw material of tissue engineering, which are seeded onto, into, or within a biomaterial, and are then

cultured using different growth factors, signals (e.g., chemical, or mechanical), or other property to properly direct tissue development. Biomaterials are typically used to create scaffolds, which serve as the initial matrix or platform for cells to grow on which will prompt different development and properties.[28] Scaffold-free tissue engineering refers to an approach where cells are used for the growth of tissues without a biomaterial scaffold. This is further categorized into self-organizing or self-assembling, with their definitions stemming from thermodynamic principles, whereby self-assembly occurs without the use of external energy or intervention and self-organization occurs with external energy or intervention.[29] Cells in scaffold-free engineered tissues adhere to each other as opposed to a biomaterial scaffold and secrete their own extracellular matrix (ECM).[30]

Scaffold-free models provide a number of benefits for the testing of engineered tissues. The lack of scaffold material allows for a direct evaluation of the condition and properties of the cells themselves, without the scaffold influencing the results. This is particularly important when performing mechanical testing, as biomaterials and scaffolds will often have significantly different material properties than the cells themselves, which may overshadow their ability to produce ECM.

The tissue model chosen for this thesis was the Rolle lab tissue ring model. The rings are a scaffold-free self-assembled model, formed through the seeding of cells into a custom-made round bottom annular single well cast in agarose. Agarose does not allow for cellular adhesion, and thus the cells in the well aggregate and form cell-cell contacts. The cells secrete their own extracellular matrix. After a culture period ranging from 7-14 days, the rings will have developed into stable and robust tissue constructs. The tissue rings themselves create their own ECM, have low sample-sample variability, mechanical stability and possess an established method for production and testing. The ultimate goal for these rings is the creation of tissue engineered blood vessels (TEBVs) created from the fusion of individual tissue rings. Once fused, the TEBVs will be used as an in vitro model of cardiovascular disease to screen potential drug candidates. The ring model serves as a promising in vitro model of disease as there are established mechanical testing criteria of annular constructs, as well as the ring form factor being conducive to measure changes in contractility.[11] Additionally, 3D cultured models have been shown to be more similar to in vivo conditions than 2D monolayers, further emphasizing the utility of the model.[25]

2.2 Cell Banking

One of the most essential components of engineered tissues, cells, represents the most resource-intensive core materials used for tissue engineering. Most tissue engineering projects can require millions to billions of cells for single experiments or products. This is the case for the creation of entirely artificial organs, which are expected to need between 1-10 billion cells for fabrication.[6] Due to the immense number of cells needed for any tissue engineering application, cell expansion is considered in the industry as one of, if not the most, expensive and time-consuming step in the process.[31] Due to the importance and necessity of cells as a core material, the creation of cell banks is a common practice.

The need for the cell bank also ensures a need for adequate supplies and reagents for their culture. Using cell banks creates a need for a robust system of organization and documentation, to maximize access to cells, standardize the approach at which they are stored, and provide more thorough and consistent data.[32] Consistency in cell banking is generally accomplished through a centralized system within larger companies, where a department is dedicated to the storage, care, and distribution of cell stocks. While this level of organization may be easier within larger pharmaceutical companies, individual labs and startup companies rely on a simpler method of distributing a master cell bank to individual groups for tissue fabrication and research.[32] While simpler it can be a detriment to consistent data across the overall organization, as the cells could be grown under different culture conditions, with different reagents, be passaged a different number of times, and be frozen using different methodology. All these different factors could cause phenotypic differences to arise between individual groups from the same original stock. Contamination within cell stocks has been problematic within cell culture with quality control testing companies reporting that as many as 18% of cell lines were found to be misidentified or contaminated, and that around 8% of cell stocks had mycoplasma infection.[32]

Several different procedures are generally put into place to act as a failsafe and to ensure proper storage conditions, this includes the creation of multi-tiered cell banks, generally consisting of a two-tiered bank using a master cell bank and a working cell bank.[33] The master cell bank contains the pure unadulterated samples that were originally developed/received and are kept in case contamination is detected in the working cell bank, or to replenish the working

cell bank, which, as its name implies is the cell bank that is used in general lab protocols. Certain companies employ larger more robust systems, such as AstraZeneca, which employs a 4-tiered system, utilizing an archive cell bank and an assay-ready cell bank alongside the working and master banks. Archive cell banks have cells stored in an alternative site, in the event the master cell bank being compromised. The assay-ready bank stores cells at higher concentrations for direct use in cellular based assays, which have reported equivalent performance to normally cultured cells.[32]

2.3 Cryogenic Banking

The fundamental concept of cell banking lies in cryobiology and cryogenic banking. Cryobiology studies the mechanics of biological systems when exposed to low temperatures, while cryogenic banking is the practice of freezing cells below physiological temperatures to halt their activity and lower the overall metabolic activity and oxygen consumption of the cells .[10,34-35] This process is a necessary procedure in the storage and handling of cells, preventing the need for continuous culture of cells, reducing overall resource and reagent usage, allowing testing and validation, and permitting shipping of samples outside of the original facility.[36] Additionally, the continuous culture of cells creates unnecessary risks such as cellular senescence, contamination from pathogens or various cell lines and the risk of phenotypic or genotypic drift.[37-40]

The clear need for cryogenic banking comes with several important considerations. Cells are extremely susceptible to internal and external damage during the freezing and thawing processes of cryogenic banking, and thus optimal conditions must be employed to maximize their survival and function. The main risk associated with cryogenic banking comes from the freezing process and the formation of ice. When left unmitigated ice crystals can form intra or extracellularly.[41] Extracellular ice formation generally occurs first and increases the extracellular solute concentration from the phase transition of water. The decreased solute concentration causes an osmotic reaction of intracellular fluid being transported across the cellular membrane.[36] This process increases the solute concentration within the cell, which can cause osmotic stress and damage. Additionally, extracellular ice crystals are capable of damaging cell membranes. Intracellular ice crystal formation, while rarer, is a product of slow freezing rate of a sample, and is generally fatal for cells, interfering with internal structures and potentially

rupturing the cell membrane.[41-42] Thus, there is an extensive body of research that has gone into diminishing these effects, the main two ways of addressing these issues are controlling the rate at which cells are frozen, as well as the use of cryoprotectant agents (CPAs).

Freezing rate is an important variable to control during cryogenic banking, as freezing samples too quickly can lead to intracellular ice formation, while freezing too slowly can lead to osmotic stress and other methods of cellular damage.[43] Due to the potential for adverse effects, it is common practice to use a controlled freezing rate of 1°C/min to minimize cell death during the process.[42]

The next method of control is the use of CPAs. CPAs are defined as "any solute which, when added to cells in their medium, allows higher post-thaw recoveries than if it were not present.[36]" The mechanism of action for CPAs is not fully understood but has been found to increase cell survival. CPAs are theorized to alter water properties and prevent the formation of ice crystals. Certain CPAs are also able to cross the cellular membrane, which reduces the osmotic stress associated with dehydration and increased solute concentrations.[44] Although CPAs allow for increased post-thaw viability, prolonged exposure has been found to have cytotoxic properties. Dimethyl Sulfoxide (DMSO), a commonly used CPA has been shown to have several detrimental effects across different cell lines, and can cause membrane dysfunction, changes in secondary structures of proteins, effects on cellular transport system, and even lowered cell growth and apoptosis.[45]

Because of these potential side effects, it is not common practice for cells to be used directly after thawing for the creation of 3D tissue constructs. In general, cells are thawed, plated, and cultured to allow for a period of recovery. However, even with a recovery period, cells can still experience cryopreservation-induced delayed-onset cell death (CIDOCD), which can affect cellular function and responsiveness days to weeks after thawing.[10] There has been little research done to assess the feasibility of using a cell bank directly from freeze for tissue manufacturing when compared to the gold standard of culturing and trypsinizing cells prior to tissue formation. However, 3D cell culture, as in scaffold-free engineered tissues, has been noted to provide several benefits to the viability, growth, and clinical relevance to the expansion of certain cells, which may indicate that cells that are directly thawed from a cell bank can be used directly for tissue formation in lieu of regular expansion of cells prior to tissue fabrication.[9,46]

Chapter 3: Materials and Methods

3.1 Cell Bank Creation

To develop the cell bank, rat aortic smooth muscle cells (RASMCs; WKY 3M-22 clonally expanded line[47-48]) were cultured in 145 mm cell culture dish in complete media, composed of DMEM (Caisson Labs) supplemented with 10% FBS(Gibco), 1% Penicillin-Streptomycin, L-glutamine, Non-essential Amino Acids, and Sodium Pyruvate (Corning Inc). Cells were grown at 37° C and 5% CO_2 for 3-4 days depending on the number of cells required for each experiment and trypsinized once the plates were ~80% confluent. Once the cells had been trypsinized and lifted off the plate they were centrifuged and concentrated at 1.1 x 10^6 cells/mL. 100 µL of DMSO was then aliquot into the appropriate number of 1.3 mL cryovials, followed by 900 µL of cell stock giving a final concentration of 1 x 10^6 cells/mL. Cryovials were then placed into a Mr. Frosty Freezing Container (ThermoFisher) and placed into a -80° C freezer overnight. The next day, vials were removed from the -80° C freezer and stored in a liquid nitrogen tank. Cell vials were kept inside liquid nitrogen for a minimum of 1-2 days before thawing. Cells thawed from this cell bank immediately prior to cell seeding for tissue ring preparation are referred to as “Freshly Thawed” (FT) samples.

3.2 Ring Seeding

To prepare the required number of “normally cultured” (NC) control ring samples, vials from the cell bank were thawed and plated 2-3 days prior to ring seeding. Vials from the cell bank were removed from liquid nitrogen, thawed, spun down at 1000 rpm for 5 minutes and had cryopreservation media aspirated and replaced with complete media to remove excess DMSO. Cells were plated in a 145 mm cell culture dish with 20 mL of complete media in each cell culture dish, which was then allowed to incubate at 37° C and 5% CO_2 until 80% confluence was achieved.

One day prior to seeding, ring-shaped agarose cell seeding wells were formed by pipetting an autoclaved 2% agarose-DMEM solution into custom, autoclave-sterilized PDMS ring mold inside a sterile biosafety cabinet as previously described in Gwyther et al[9]. Agarose

was allowed to cool for 5-10 minutes after which individual ring molds were removed aseptically, placed into a 48-well plate, and incubated with complete medium overnight at 37° C and 5% CO_2. Prior to cell seeding, media was aspirated from the ring wells before cell suspension was seeded into each well.

On the day of ring seeding NC cells were trypsinized, resuspended, and concentrated together in a 15 mL conical tube. Following resuspension, cell bank vials for the FT rings were removed from liquid nitrogen, thawed, spun down at 1000 rpm for 5 minutes, and resuspended in complete medium to remove DMSO and pooled together in a 15 mL conical tube. After cells from both groups (NC and FT) were collected, the conical tubes were agitated to ensure re-suspension, and a 200 µL sample of each was collected and analyzed on a NucleoCounter NC-200 using an AO/DAPI assay to assess cell viability and total cell concentrations (Figure 1). Results were collected and saved in a report. After taking the initial cellular viability measurements, NC and FT cells were spun down at 1000 rpm for 5 minutes once more and concentrated at 1 x 10^7cells/mL.

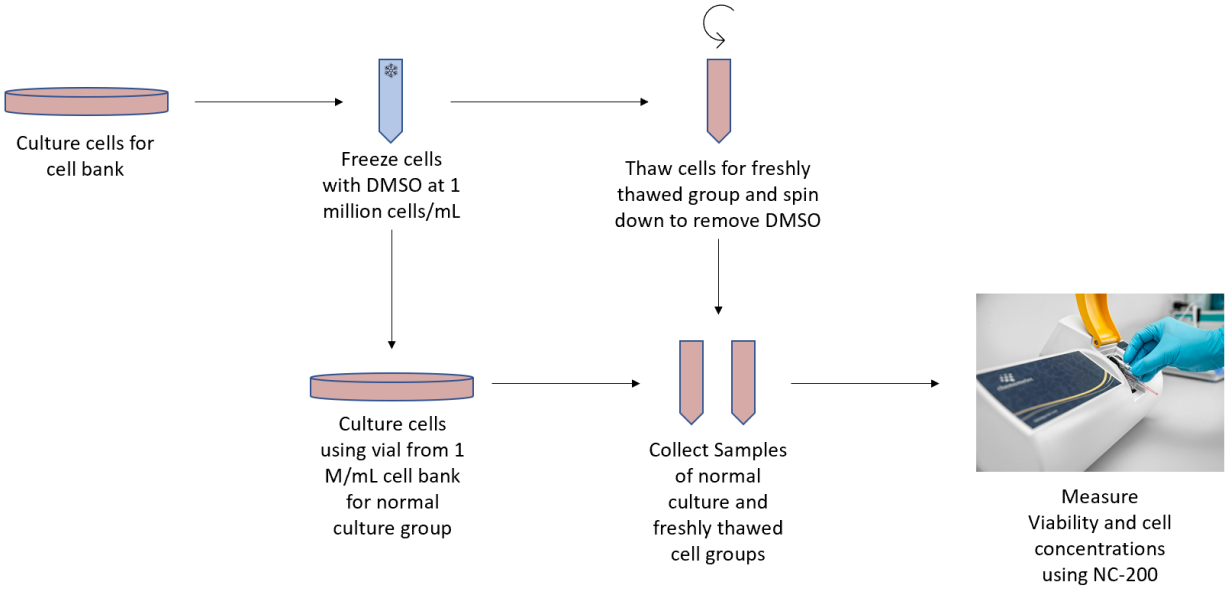

Figure 1: Overview of cell viability testing procedure used prior to tissue ring seeding

Once concentrated 50 µL (500,000 cells) were dispensed into each agarose mold for both NC and FT groups. After seeding both groups, enough complete media was put into each well so that it reached ~½-¾ the height of the agarose mold to prevent cells from spilling out of the

mold. The 48 well plates were then incubated overnight at 37° C and 5% CO_2. The next day, media was aspirated outside of the agarose mold and carefully flooded with 400µL of complete medium to cover the ring mold. Rings were imaged daily at 2x magnification on an inverted microscope with daily media exchanges performed. After seeding was performed the rings were cultured for 7 days (Figure 2), with all remaining assays performed throughout the 7-day incubation as described in Figure 3.

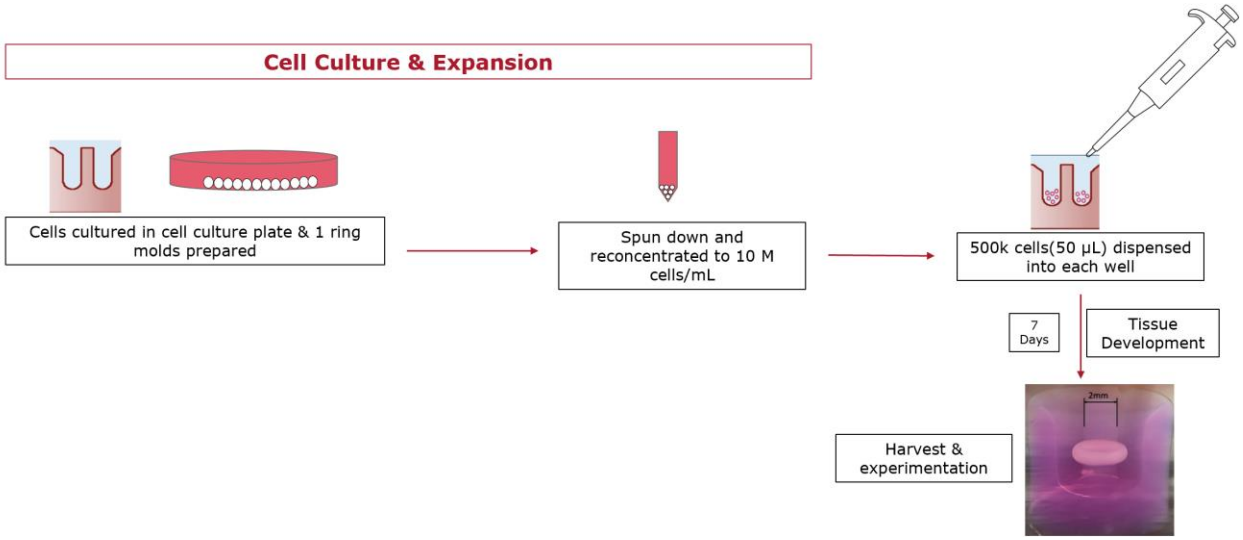

Figure 2: Overview of workflow used to create tissue rings

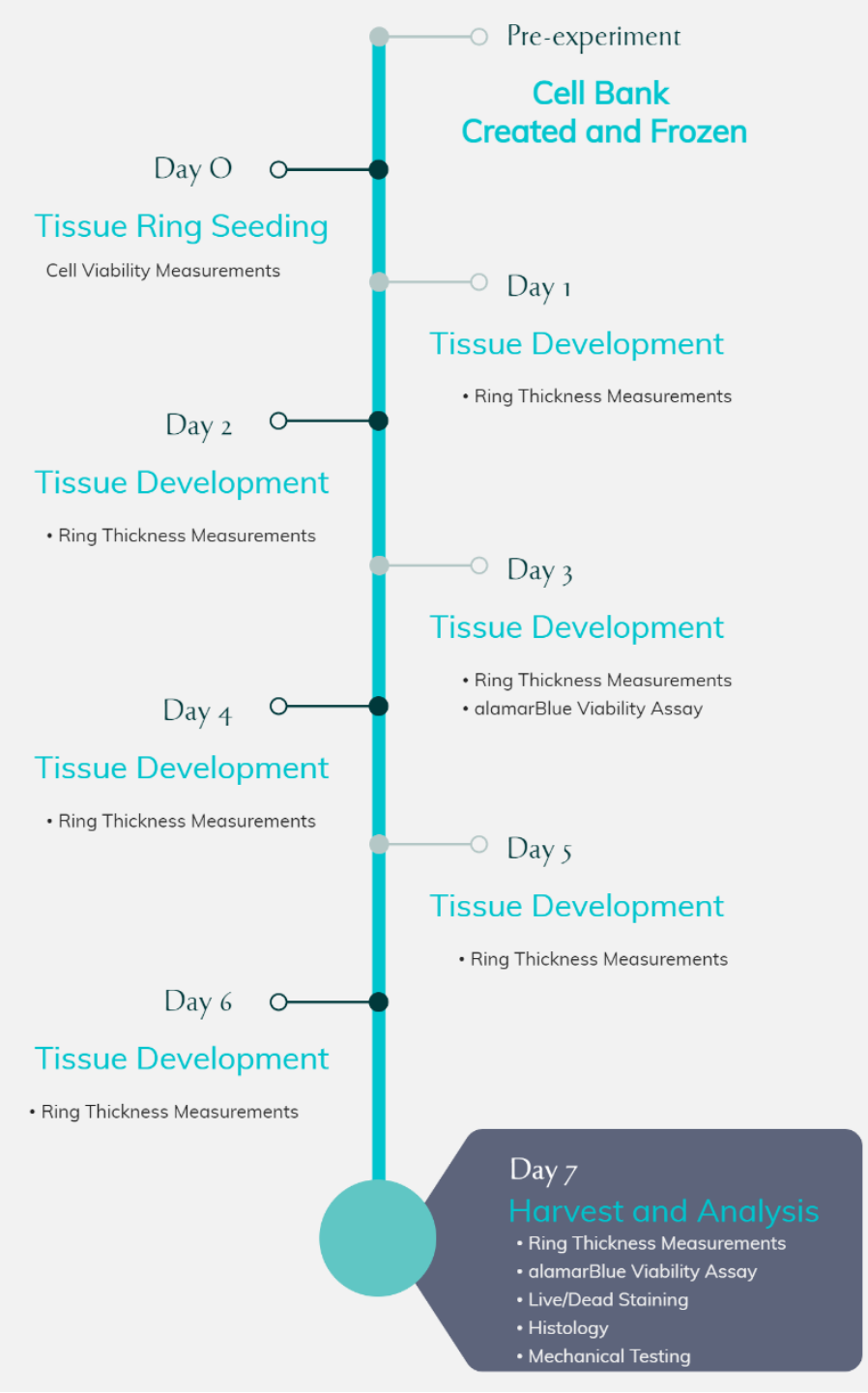

Figure 3: Timeline of tissue ring preparation and experimentation

3.3 Ring Thickness Measurements

Images of the rings were saved as .tif files and processed on ImageJ using the wand tool (Figure 4). An estimate of the outer and inner areas of the ring were obtained and recorded. Following data collection, the outer and inner areas were converted to radii using the equation:

$$Radius = \sqrt{\frac{area}{\pi}}$$

The inner radius was subtracted from the outer radius to estimate thickness. This process was repeated each day for each ring sample imaged.

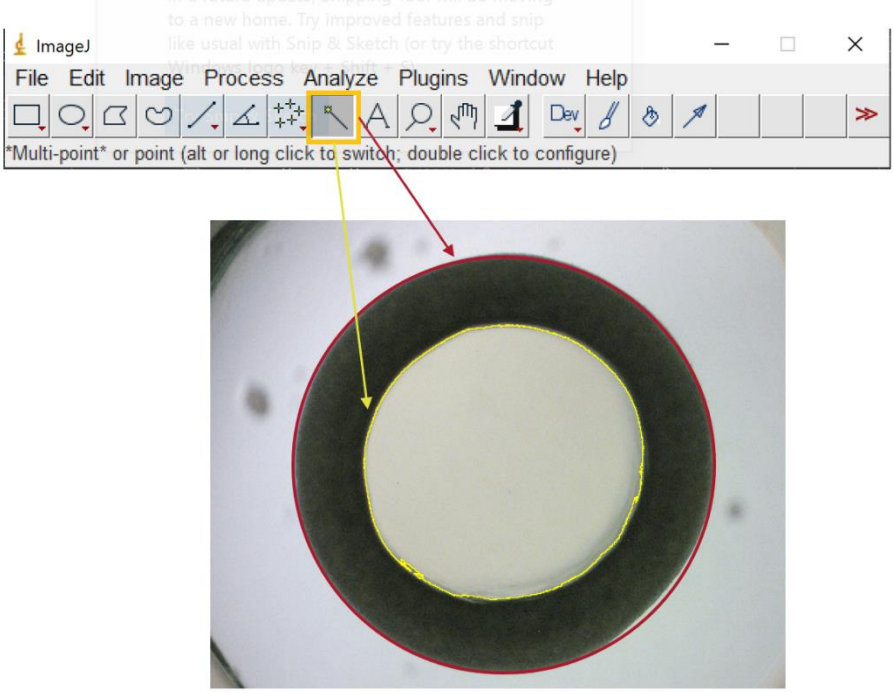

Figure 4: Image showing example usage of ImageJ wand tool to estimate the inner and outer areas of the tissue rings

3.4 Histology

On Day 7, 2-3 rings from both the NC and FT groups were removed from culture and placed into a new 48 well plate. The tissue rings were then fixed in 10% neutral buffered formalin for 1 hour. Fixed rings were removed from their molds and placed into a tissue processing cassette in 70% ethanol. Samples were processed, embedded in paraffin, and sectioned in 5 µm slices and adhered to charged slides. After processing slides were incubated at 50° C for 1 hour then stained with Hematoxylin & Eosin (H&E) to observe overall morphology

and Picrosirius Red/Fast Green (PRFG) to observe collagen production as described in Gwyther et al[9].

3.5 alamarBlue

A 10% alamarBlue (AB) solution was made prior to beginning the assay. Total volume was calculated under the assumption that the agarose well constituted a volume of ~300 µL, to give a total well volume of 1 mL. Each well was carefully aspirated using a 1 mL micropipette to remove old media from each ring well. After removing media from each ring well, 700µL of AB solution was placed into each ring mold well. Additionally, AB solution was placed by itself into an empty well to act as a blank/negative control, as well as wells containing 100,000, 250,000, 500,000, and 1,000,000 cells in 2D monolayers which had been plated overnight. Following seeding, the 48 well plates were placed back in the incubator for 8 hours. After 8 hours of incubation 50 µL of AB solution was then taken from each sample and placed into an empty 96 well plate. The 96 well plate was then placed into a PerkinElmer Victor 3 plate reader and read at 540 nm excitation and 590 nm emission wavelengths using a premade AB protocol. Data were then saved as a .xls file for later analysis.

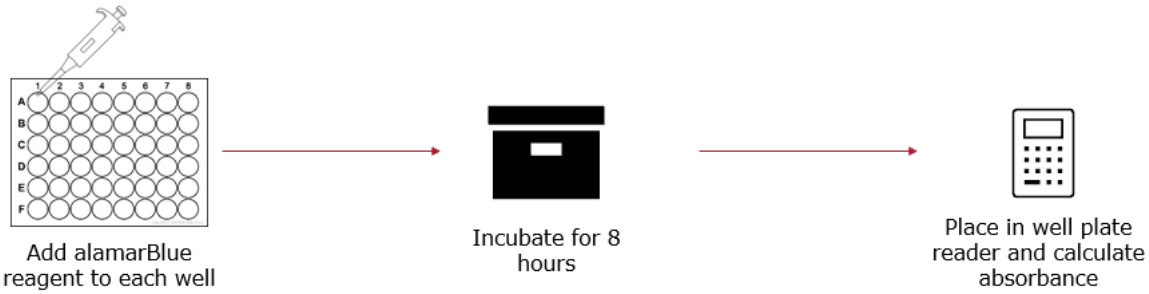

Figure 5: Summarized procedure of alamarBlue assay

3.6 Live/Dead

Live/Dead staining, consisting of Calcein AM and Ethidium Homodimer (Invitrogen), was conducted on 2 samples of each experimental group. Stock reagents at concentrations of 4 mM and 2 mM Calcein AM and Ethidium homodimer respectively were removed from storage and incubated at room temperature for 30 minutes. Following the reagent preparation, a working

solution of 2 µM Calcein AM and 3 µM Ethidium homodimer in PBS (-) was created. 200µL of working solution was pipette into fresh 96 well plate wells. Rings from NC and FT groups were then removed from their agarose molds and placed into the Live/Dead solution. The plate was then placed into the incubator for 90 minutes to allow for penetration into the ring. After incubation, samples were imaged at 4x magnification with green and red fluorescent filters using a Keyence BZ-X800 fluorescent microscope.

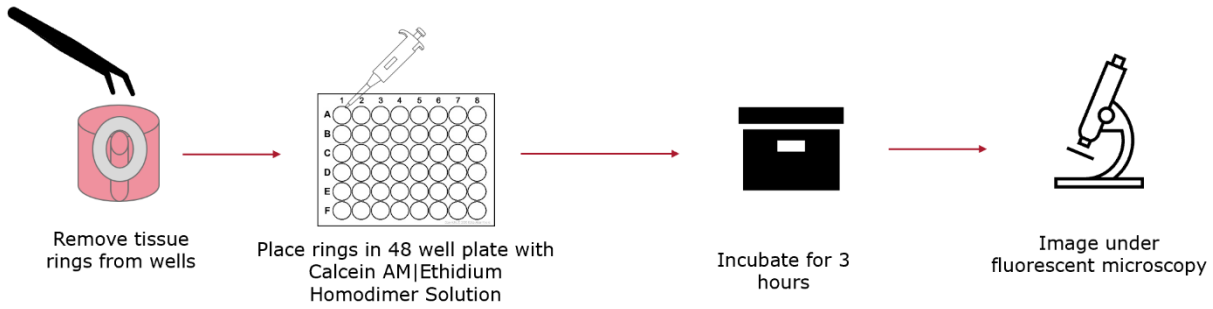

Figure 6: Summarized procedure used for fluorescent live/dead imaging of tissue rings using Calcein AM and Ethidium Homodimer

3.7 Mechanical Testing

Samples used for the AB assay were removed from their molds and used for subsequent mechanical testing. An Instron E1000 with custom sample metal wire sample mounts was used to perform ultimate tensile stress (UTS) measurements of ring samples. Mounts were submerged in PBS, and ring samples were manipulated onto the top of the wire mount. The estimated area derived from ImageJ was input into the program and the ring was stretched until a tare load of 1 mN was reached. Following the stretching of the ring, the Instron ran a preloaded program, where the sample was pre-cycled then stretched at a constant rate of 10 mm/min until failure. Failure strain, UTS data were collected on the machine and saved for subsequent analysis.

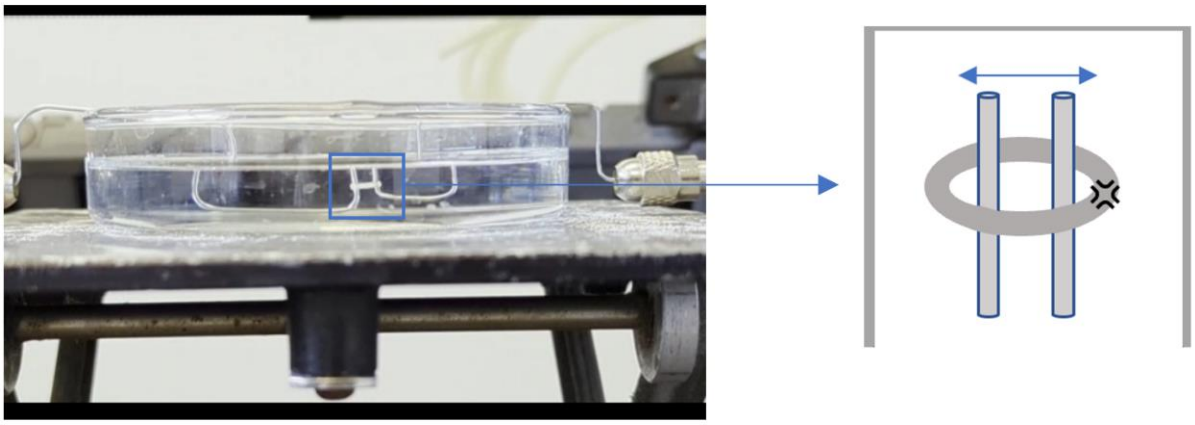

Figure 7: Tissue Ring mounted onto custom sample wires prior to sample being stretched until failure

3.8 Statistical Analysis

Data were analyzed using GraphPad Prism 9.5.1., and post-hoc power analysis was performed using G*Power 3.1.9.7. The method of statistical testing was determined after performing normality testing and a comparison of standard deviations. Initial cellular viability was analyzed using a 1-tailed Welch's t-test due to unequal standard deviations. AlamarBlue data were analyzed using one-tailed Mann-Whitney U tests when the dataset did not have a normal distribution, and unpaired t-tests when the dataset had a normal distribution. Ring thickness measurements were analyzed using mixed-effects analysis with Sidak's multiple comparisons test and mechanical properties were analyzed using one-tailed unpaired t-tests. One tailed testing was performed as adverse effects were hypothesized to give decreased performance in alamarBlue and mechanical tests. A two tailed test was used for ring thickness as it was hypothesized that the use of FT tissue rings could increase or decrease the thickness measurements.

3.9 Sample Size Calculations and Power Analysis

The overall null hypothesis in this study is that FT tissue rings will not be statistically different in thickness, nor will it be statistically inferior in metabolic activity, and mechanical strength compared to NC tissue rings. As this thesis seeks to not reject the null hypothesis, there

must be sufficient evidence to account for the chance of Type II error. Therefore, a statistical power analysis was performed using values obtained from preliminary experiments to determine the ideal sample size needed to achieve a statistical power of ≥ 0.8. This value evaluates the likelihood of falsely failing to reject the null hypothesis, with a power of 0.8 indicating there is an 80% likelihood that the data did not occur by random chance.

The achieved power of the cumulative experiments was calculated using G*Power, through a reordering of Equation 1, shown below. These values were obtained using the sample sizes in each group, the calculated p-value, and the effect size, as shown in Equation 2 and Table 1. The final testing sample number was determined through a post-hoc analysis using the initial effect size and p-values obtained in preliminary experiments. Post-hoc analysis was done for each testing criteria to determine what test required the most samples. However, given the presence of artifacts in area and thickness data, analysis by Gwyther et al.[11] was used to determine sample size required to obtain statistical power of ≥ 0.8 for thickness. The final sample size was chosen after calculating the individual sample sizes required to achieve statistical power ≥ 0.8 for each individual preliminary experiment. The largest sample size required was found to be 18 total samples. To account for potential issues or loss of samples during testing, 48 total samples were included for the final comprehensive tests comparing NC and FT ring properties.

$$n_i = 2\left(\frac{Z_{1-\propto/2} + Z_{1-\beta}}{ES}\right)^2$$

Equation 1: Calculation of sample size; n_i = sample size, $Z_{1-\propto/2}$ is the normal standard distribution for desired confidence level, $Z_{1-\beta}$ is the standard normal distribution for desired power level (1.96 + 0.84 for α=0.05 and β=0.8), ES is the effect size.

$$ES = \frac{|u_1 - u_o|}{\sigma}$$

Equation 2: Calculation of effect size where u_1 = mean of test group values, u_o = mean of control group values and σ = pooled standard deviation

Table 1: A priori statistical mean and standard deviation values used to find the effect size of initial experiments

A priori (Power = 0.8)	μ_1(NC)	μ_0 (FT)	σ_1 (NC)	σ_0 (FT)
AlamarBlue	229000	211000	39600	23900
(UTS)	16.4	14.02	3.62	3.60
Failure Strain	1.23	1.30	0.410	0.449
Maximum Tangential Modulus (MTM)	14.0	11.4	2.79	4.21

Chapter 4: Results

Experimental analysis of NC and FT tissue rings was conducted as a series of six experiments, consisting of 7-day ring culture. Four experiments included 12 rings in each group and two experiments included 24 rings in each group, for a total of 192 ring samples analyzed during the course of this thesis project. The studies were performed in two phases – initial experiments (Experiments 1-5) were performed to iterate on experimental design and generate data for power analysis. Experiment 6 included 48 samples (n = 24 per group, NC v. FT rings). The outcomes measured per experiment can be seen in Appendix 1.

4.1 Initial Cell Viability

Prior to ring seeding, the initial viability of cells used to prepare the Normally Cultured (NC) and Freshly Thawed (FT) tissue ring sample groups was analyzed. The initial viability of the FT cells was lower and more variable than the NC cells, ranging from 89.6-95.3% viable and 99.6-99.9% viable, respectively. The mean values calculated during testing were 92.5 ± 1.84 % viability for FT cells and 99.8 ± 0.12% viability for NC cells. The observable, statistically significant difference between the two groups, shown in Figure 8, is to be expected, as the cells taken for the NC group were rinsed with PBS prior to trypsinizing, which would have removed most dead cells in solution. Additionally, freezing is known to impact cell viability, so a small amount of cell death was hypothesized in the FT group.

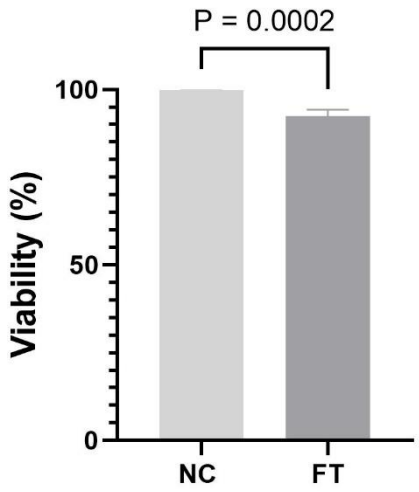

Figure 8: Bar graph showing the difference in percentage of viable cells analyzed from NC and FT tissue ring sample groups (values are expressed as mean ± SD, n = 6, p = 0.0002)

4.2 Ring Formation

To quantify tissue stability, the tissue rings were monitored for their ability to successfully form tissue rings and remain stable over the 7-day culture period. For this analysis, a successful tissue ring formation was defined as a ring that had full fusion to itself around the agarose post and a ring that does not have any extremely thin areas, with examples of failed rings being shown in Appendix 2. Initial experiments did not record tissue formation rate, therefore a total of 120 rings were included in the tissue ring analyses. In total 51/60(85%) rings successfully formed for the FT groups while 7/60(11.6%) rings failed to form, the remaining 2(3.3%) rings were compromised during handling and could not be observed for the full 7-day culture. For the NC group 55/60(91.6%) rings formed, 4/60(6.6%) failed to form and 1(1.6%) was compromised during handling. As a result, 55 NC rings and 51 FT rings were initially included in the analyses. Most rings that had formed on the first day remained intact over the 7-day period, as seen in Appendix 3, and both groups appeared visually identical on day 7 as seen in Figure 9.

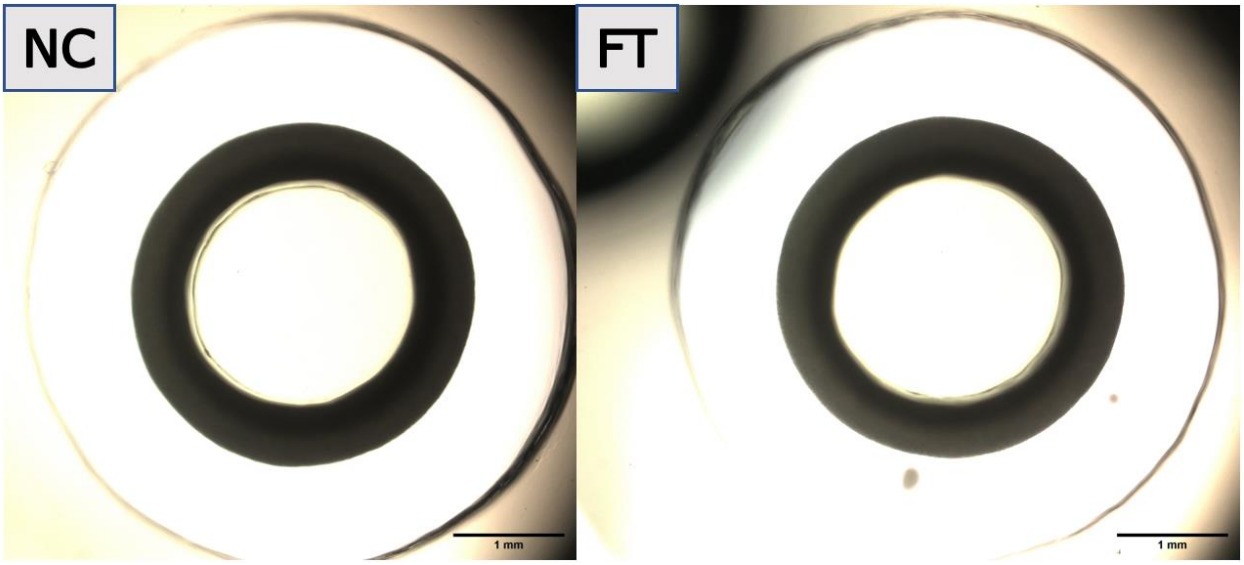

Figure 9: Examples of fully formed tissue rings on day 7(Left image shows a NC tissue ring, and right image shows a FT tissue ring, 1mm scale bar shown in bottom right of both images)

4.3 Tissue Ring Thickness

Images of tissue rings were recorded daily to analyze ring formation and measure ring thickness between the two experimental groups. In total, images were acquired from 120 ring samples over their 7-day growth period, after excluding invalid or compromised samples, this represents 45 NC rings and 44 FT rings observed over 3 experiments. The average thickness values for the 7-day period are recorded in Appendix 4 and plotted in Figure 10.

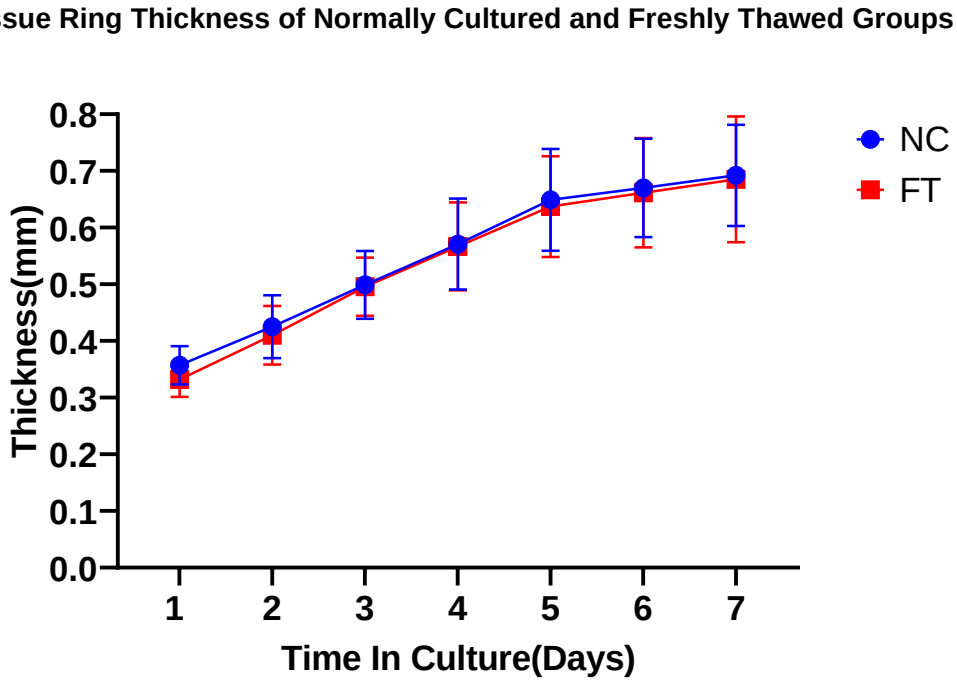

Figure 10: Thickness measurements charted over 7-day tissue formation period for NC (n=23-46) and FT (n=28-46) tissue rings (variable sample size were used each day due to corrupted image files, sample loss, or poor image quality preventing analysis)

As can be seen from Figure 10, NC and FT groups follow the same overall trend for thickness with no statistically significant differences in mean values at each time point. A mixed-effects analysis of treatment and time with Sidak's multiple comparisons test was performed on the data to determine if there was a statistically significant difference between NC and FT groups on every day of culture and to account for Type I error inflation. The analysis showed a lack of significantly different values between the NC and FT groups. The Sidak-adjusted p-values are shown in Appendix 4 showing that each day had a p-value larger than >0.05 with day 1 having the smallest p-value at 0.0581 and days 3, 4 and 7 having a p-value >0.9999. Additionally, the mixed effects analysis found that the mean ring thickness for NC and FT rings on each day were statistically significant from the mean values measured on every other day with a p-value <0.0001. In other words, thickness was significantly greater on day 2 than on day 1 for both groups, although the mean thicknesses of FT and NC rings were not significantly different from each other on any given day.

4.4 AlamarBlue Assay

Metabolic activity measurements using an alamarBlue assay were performed to quantify tissue stability and viability. The assay was applied across all six experiments, however only data from three experiments were included in the final analysis.

The first experiment used a destructive testing method, where rings from each group were removed from their agarose wells and placed into a 10% AB solution in a new 48 well plate and incubated for 4 hours. This destructive method was done to increase the surface area of the tissue ring to the AB reagent and to account for the slow diffusion of solution through the agarose mold. A negative control (containing AB reagent and media) and positive 2D monolayer control (containing 1M seeded cells), were used to show the baseline and saturation points, respectively. The results from this testing showed similar readings, as seen in Figure 11. For ease of reporting values were converted to %reduction of alamarBlue when compared to the positive control. The NC and FT tissue ring groups had values of 63.3 ± 5.00% and 63.6 ± 7.69% reduction, respectively. When analyzed with an unpaired t-test the groups were found to not be statistically significant, with a p-value of 0.5316.

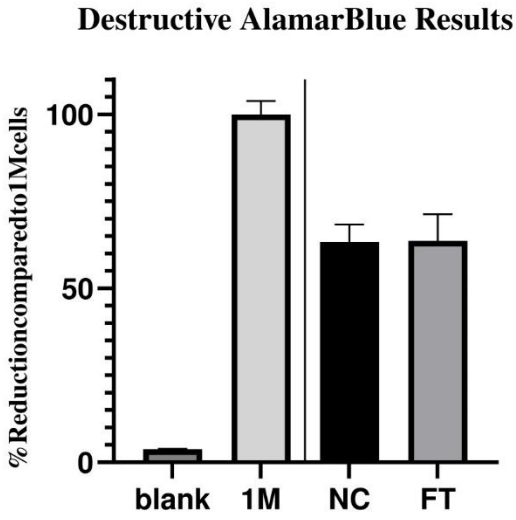

Figure 11: Bar graph of alamarBlue assay for experiment 5 depicting average metabolic activity (measured as a %reduction compared to 1,000,000 plated cell control) between NC and FT groups after 4 hours (p = 0.5316). (Blank shows the reading of a well with no cells and positive control used 1M cells to reach alamarBlue saturation) (n = 8; NC) (n =4; FT)

The next two alamarBlue runs were performed as described in the methods section on the sixth experiment on days 3 and 7 to determine if there was an initial lowered viability and subsequent recovery of the FT tissue ring group. Additionally, a negative control in the form of a blank, consisting only of AB solution was included. Cells plated in individual wells at different concentrations were again used as positive controls to determine the saturation points, as well as to quantify the level of activity relative to the tissue ring samples.

Measurements taken on day 3, as seen in Figure 12 and Appendix 5, showed higher NC values compared to the FT group. For ease of reporting, values were converted to %reduction when compared to the 100,000 plated cell control. The NC group averaged 58.8 ± 25.5 % reduction and the FT group averaged slightly lower at 45.6 ± 19.0% reduction. These values proved to have a statistically significant difference when analyzed using a one-tailed Mann-Whitney U test, which was used due to an absence of normal distribution, with a p-value of 0.0179. The measurements from day 7, shown and summarized in Figure 12 and Appendix 5,

showed the FT rings having slightly higher %reduction and absorbance readings. When converted to %reduction compared to the 100,000-cell control, the FT tissue rings had 82.2 ± 12.0 % reduction compared the NC tissue rings which averaged at 76.9 ± 8.97 % reduction. However, when the AB values between the NC and FT tissue rings were analyzed with a one-tailed unpaired t-test the two groups were found to not be statistically different, with a p-value of 0.9405.

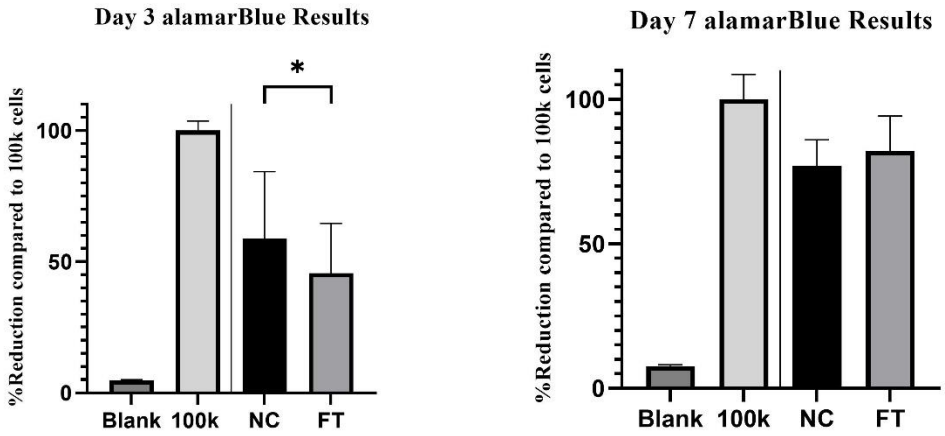

Figure 12: Bar graphs of alamarBlue assay on days 3 and 7 of experiment 6 depicting average metabolic activity between NC and FT groups and control groups with 0 and 100,000 cells after 8 hours (Measurements are represented as %reduction compared to plated 100,000 cell control) (Day 3 | p = 0.0179; n =21 for both NC and FT) (Day 7 | p=0.9405; n =21 and 20 for NC and FT respectively)

4.5 Live/Dead Stain

Live/Dead staining with Calcein AM and Ethidium Homodimer was performed to qualitatively analyze cell viability within the tissue rings formed from NC and FT cells. Figure 13 shows a representative view of the two groups, where green represents live cells and red represents dead cells. There were no major visual differences between the two groups regarding live or dead cell labeling. The assay was conducted on NC and FT tissue rings in three of six experiments, with no visual differences. In the third run of this experiment, we were unable to

clearly visualize the ethidium homodimer, as the samples were first used for metabolic analysis by alamarBlue, which resulted in residual background fluorescence.

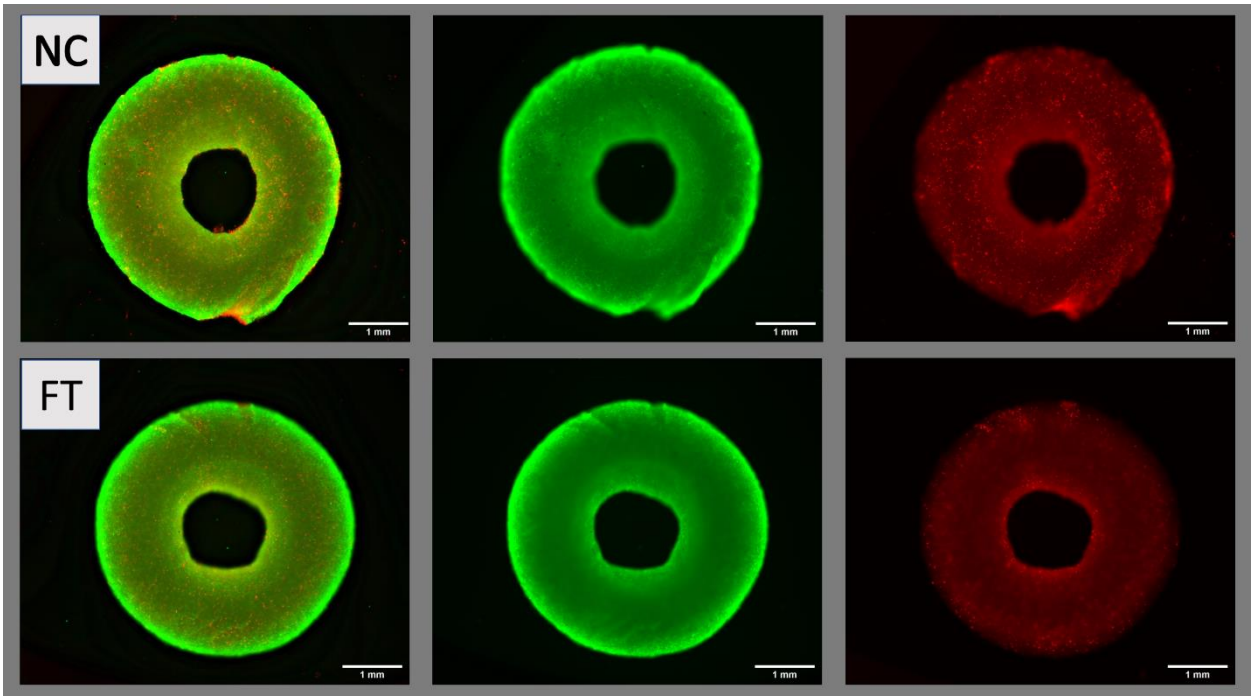

Figure 13: Live Dead Staining of NC (top ; n=4) and FT (bottom ; n=4) tissue rings after 3 hours of incubation showing no major visible differences (column 1 shows the overlayed channels, column 2 shows the Calcein AM (live) staining channel, and column 3 shows the ethidium homodimer (dead) staining channel, 1 mm scale bars are shown in the bottom right of each image)

4.6 Histological Analysis

To visualize tissue ring morphology histological stains of Picrosirius Red/Fast Green (PRFG) and Hematoxylin and Eosin(H&E) were run on most experiments. Images of H&E staining, obtained using a Nikon Eclipse TS100, are shown at 4x and 10x in Figure 14. Both NC

and FT tissue rings appear visually identical in terms of cellular orientation, density, and overall structure.

Images of PRFG staining are shown at 4x and 10x in Figure 15, also appear to have no major structural differences in terms of collagen formation and inner ring morphology, with both rings showing heavy interior collagen production, and an outside boundary layer with little deposited collagen.

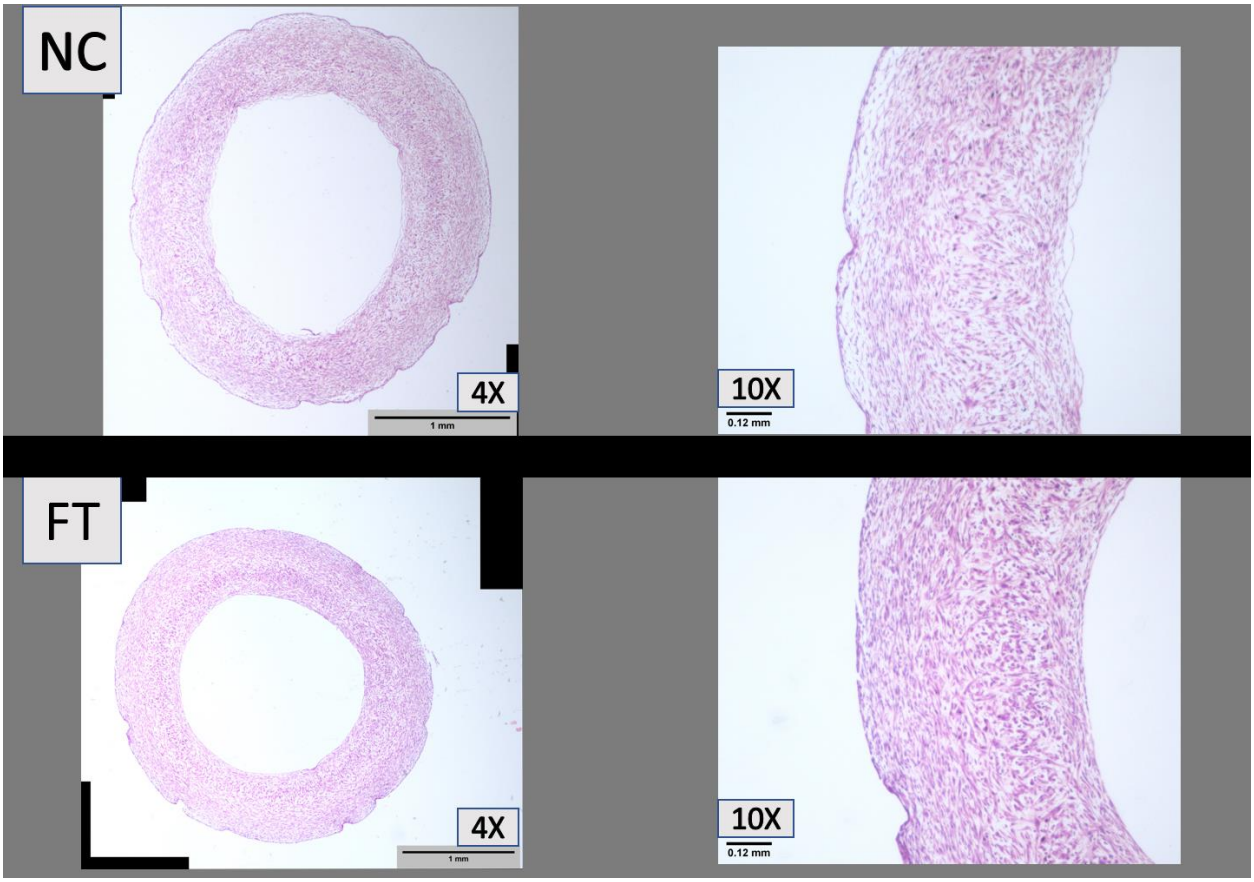

Figure 14: H&E staining of NC (top) and FT (bottom) tissue rings depicting visually similar cellular density and structure between both groups. Images are shown at 4x magnification(left) and 10x magnification(right). Nuclei are dyed purple while cytoplasm is dyed pink. Scale bars of 1 mm are in the bottom right corner of the 4x photos and scale bars of 0.12 mm are in the bottom left corner of 10x photos.

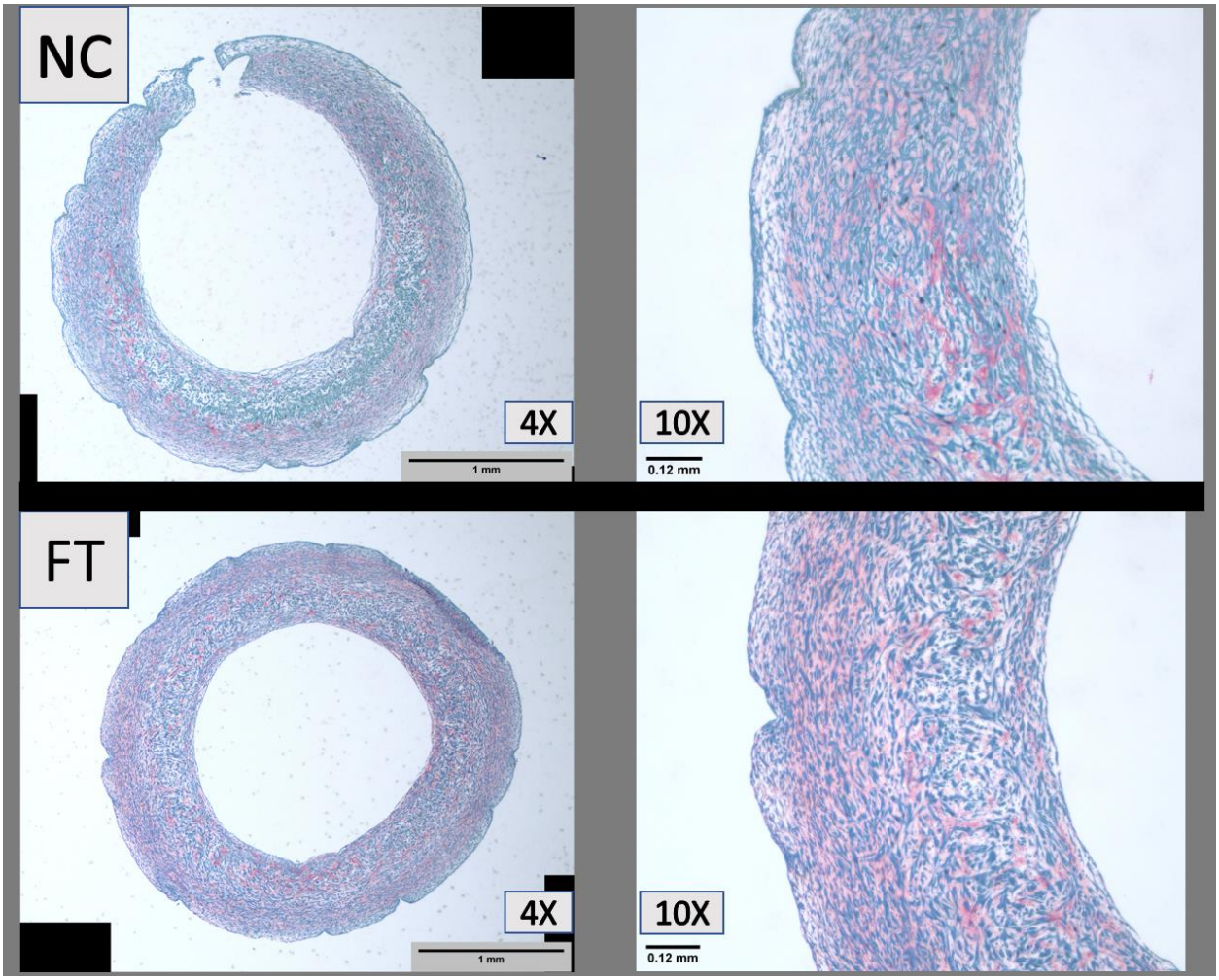

Figure 15: PRFG staining of NC (top) and FT (bottom) tissue rings depicting similar collagen production between both groups. Images are shown at 4x magnification(left) and 10x magnification(right). Collagen is dyed red and green counterstains all non-collagenous protein. Scale bars of 1 mm are in the bottom right corner of the 4x photos and scale bars of 012 mm are in the bottom left corner of 10x photos

4.7 Mechanical Testing

Uniaxial tensile testing was performed to analyze the mechanical robustness of the tissue rings. Failure strain, UTS, and MTM were the evaluated characteristics used to quantify the mechanical properties of the tissue rings (shown in Figure 16). The data for the NC groups included an average failure strain of 2.88 ± 0.644, an average UTS of 22.4±5.09 kPa, and an average MTM of 7.98 ± 1.82 kPa. In comparison the FT group had an average failure strain of 3.30 ± 0.609, an average UTS of 30.2 ± 5.32 kPa, and an average MTM of 9.50 ± 1.51 kPa (values summarized in Appendix 6). A one-tailed unpaired t-test was used to analyze statistical significance, which calculated p-values of 0.493, 0.9995, and 0.9854 for failure strain, UTS, and MTM, respectively. These results indicate that there is no statistically significant difference in failure strain, UTS or MTM values between the NC and FT tissue rings.

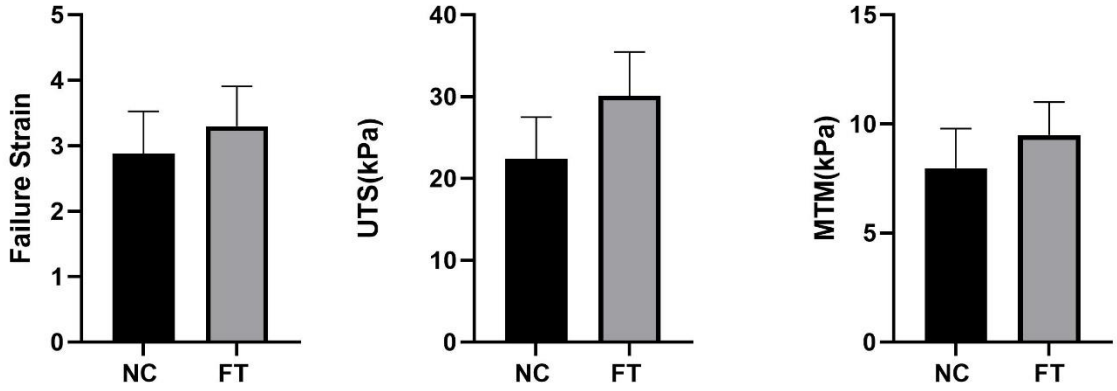

Figure 16: Bar graphs comparing mechanical values of NC and FT tissue rings. Values are expressed as means ± SD (n of NC = 11, n of FT = 15). Failure strain (left; NC = 2.88 ± 0.644, FT =3.30 ± 0.609), ultimate tensile stress (middle; NC =22.4 ± 5.09, FT = 30.2 ± 5.32) and MTM (right; NC =7.98 ± 1.82, FT = 9.50 ± 1.51) of NC and FT tissue rings

4.8 Power Analysis

Statistical analysis was performed to account for any Type II error via post-Hoc power analysis and can be seen plotted in Table 2 alongside the p-values calculated for each test. The achieved power and p-value varied from method to method, with only initial cell viability and

UTS measurements having a power ≥ 0.8. These results suggest that only initial cell viability, and UTS were sufficiently powerful to account for the possibility of Type II error.

Table 2: P-Value and Power results across all performed testing. Highlighted cells represent results that followed the predicted outcomes. Statistical significance and sufficient power are $p < 0.05$ and Power ≥0.8 respectively.

Test	p-value	Power	Statistically Significant	Sufficiently Powered
Viability	0.0002	0.998	Yes	Yes
aB Destructive	0.5316	0.0583	No	No
aB Day 3	0.0179	0.591	Yes	No
aB Day 7	0.9405	0.463	No	No
Failure Strain	0.493	0.501	No	No
UTS	0.9995	0.978	No	Yes
MTM	0.9854	0.731	No	No
Thickness Day 1	0.0581	0.05	No	No
Thickness Day 2	0.7494	0.265	No	No
Thickness Day 3	>0.9999	0.0574	No	No
Thickness Day 4	>0.9999	0.0566	No	No
Thickness Day 5	0.9949	0.0969	No	No
Thickness Day 6	0.9995	0.0738	No	No
Thickness Day 7	>0.9999	0.0622	No	No

Chapter 5: Discussion

The research aims of this thesis were to evaluate the ability of freshly thawed (FT) cells to successfully form tissue rings that mimic the structure, metabolic activity, and mechanical strength of cells that were cultured normally (NC) and trypsinized immediately prior to tissue ring formation.

Aim 1 focused on analyzing freshly thawed cells' ability to successfully form tissue and retain the same stability and structural properties as normally cultured control cells. This aim was measured via thickness measurements taken each day over a period of 7 days, as well as a viability and metabolic activity assay to evaluate tissue viability.

Results from the pre-seeding cellular viability measurements went as hypothesized, with a small, but statistically significant reduction in cellular viability in the freshly thawed cells compared to the normally cultured cells. An initial reduced viability is expected, as the freezing process and exposure to DMSO leave the cells vulnerable to ice crystal formation or the sudden uptake of water once cells are thawed, both of which can damage the cell membrane and cause cell death. Also, the freshly thawed cells may be more susceptible to mechanical damage, due to increased osmotic stress, stemming from the centrifuge used to remove DMSO prior to cell seeding.[49] However, the lowest FT viability was 89.6%, which is still capable of providing an ample number of cells for tissue formation.

Results from alamarBlue analysis were more challenging to interpret. The assay was performed two separate ways, with the first being a destructive test, where rings were removed from their molds and incubated directly in AB solution. This method allowed for the tissue rings to have a greater exposure of alamarBlue and a faster assay time, taking 4 hours instead of the usual 8 to achieve sufficient signal development. However, using this method can compromise the use of tissue rings for mechanical testing as removing the mold may have caused tissue contraction from the absence of the agarose post. The other AB method incubated the ring in the mold with AB solution for 8 hours. While this method allowed for non-destructive testing, and thus the ability to subsequently conduct mechanical testing, it had a number of drawbacks. The largest issue stemming from this method is the lowered absorbance readings from the tissue rings, likely caused by the slow rate at which AB solution can pass through the agarose mold and the smaller surface area of the tissue ring that AB can interact with. This slow diffusion may also

contribute to less accurate absorbance readings due to a lack of homogeneity of the analyzed AB solution. The other issue identified from this method was the large visual difference in the pigmentation of individual wells within each group, which was determined to be caused by cellular growth in the background of the well plates contributing to reduction of the alamarBlue assay and creating artificially higher signals. The background cell growth may explain why the NC tissue rings had a significantly higher absorbance reading for day 3 of experiment 6, as 8 wells in the NC group were found to have visible cell growth in the background, while only 4 wells in the FT group were found to have visible cell growth in later imaging. Before the day 7 alamarBlue assay, rings were transferred to a new 48 well plate to prevent artificially inflated signals. The absorbance readings from the day 3 alamarBlue assay can be seen in Appendix 5. Future AB assays should utilize a new 48 well plate prior to incubating the tissue rings, as cell growth in the bottom of the wells was shown to affect the results.

The initial destructive AB method developed similar values between the NC and FT tissue rings however had a notably lower sample size of 8 NC tissue rings and 4 FT tissue rings. The calculated p-value of 0.5316 shows that there is no statistical difference observed between the two groups and suggests that there is no loss in ultimate tissue viability after 7 days of tissue culture.

The AB assay from day 3 of experiment 6 suggested that there was an initial recovery period for the FT tissue rings, as the absorbance values were lower than the NC tissue rings and were statistically significant with a p-value of 0.0179. However, this data may simply be giving artificially inflated absorbance readings of the NC tissue rings, as stated earlier, due to the discovery of 8 NC wells having cell growth on the bottoms of the culture wells. This cell growth could explain the discrepancy between the two groups, as only 4 FT wells had cell growth in the background. The alamarBlue assay performed on day 7 of experiment 6 showed no statistically significant results with a p-value of 0.9405.

The lack of statistically significant day 7 end-point measurements of AB suggests that freshly thawed cells can rapidly recover and develop into functional tissues with similar viability to normally cultured cells that have been cultured several days prior to tissue formation. The collected AB data is a promising initial result, however, to quantify a recovery period, further work would need to be done to account for the discrepancies noted above. The freshly thawed group's ability to recover and form functional tissue may stem from 3-D constructs providing

more protection and higher rates of cell survival when exposed to toxic reagents.[9,46] Additionally, literature discussing the adverse effects of cryoprotectants such as DMSO tends to have prolonged exposure times to DMSO or immediate use of the thawed cells, whereas the culturing of FT cells into an engineered tissue still allows for recovery development[35]. The lack of a significant difference between the AB results for NC and FT tissue rings would suggest that the use of freshly thawed cells for tissue engineering would be a viable method of accelerating the overall workflow, as the cells would have a natural tendency to recover at faster rates than expected in the 3D environment within engineered tissue.

The other measure assessing viability was the use of Calcein AM and Ethidium Homodimer live/dead staining. The images across all three experiments were visually indistinguishable from one another and seemed to show slightly higher dead staining signals from the normally cultured tissue rings. The lack of concentrated dead regions or higher dead signals from the freshly thawed tissue rings suggests that there was no difference in tissue development or overall final viability. Additionally, one experiment was unable to generate an accurate dead signal, as the method was performed following an alamarBlue assay, which was found to interfere with ethidium homodimer fluorescent imaging. Future analysis should have samples set aside that are not affected by the AB reagent or have been sufficiently washed prior to analysis.

The last, and most robust set of data collected for aim 1 were the thickness measurements across 7 days, with 120 total initial tissue rings. However, a number of tissue rings that were initially seeded were excluded from final analysis due to incomplete ring formation or accidental dispensing of cell suspension into the back of the well, which caused the growth of cell debris and restricted growth of the tissue rings. Incomplete ring formation may have come from factors such as improper dispensing of cell suspension into the agarose wells, which may have caused an uneven spread of cells into the well. Additionally, improper handling may have damaged the wells and introduced agarose artifacts, both possibilities can be seen in Appendix 7, depicting an image of an unformed ring with an unidentified artifact inside of the well. Accounting for the loss of samples, the total analyzed data came out to be 593 total images and 1186 total measurements. Measurements obtained across the 7 days showed a consistent trend across both NC and FT tissue rings. For each day both groups were found to have no statistically significant difference in their data sets, with 5/7 days having a Sidak-adjusted p-value ≥ 0.99. A mixed

effects analysis was performed to better analyze the changes over 7 days and given the high sample size, an adjusted p-value was used to lower the chance of Type I error inflation. These results suggest that there is no discernible statistical difference in thickness between the two groups and is a promising indicator that there were no detrimental effects of using freshly thawed cells for tissue ring formation.

Both tissue ring groups encountered small cell spheroids forming within the agarose wells next to the tissue rings, as shown in Figure 17. The reason for their development is unclear, however, they appeared in both NC and FT cultures, suggesting that it was not a byproduct of the freshly thawed cells. One possible cause is the use of older agarose for the wells, which may have dehydrated or contained small imperfections or divots in the surface after being dispensed to form the ring well, allowing for small amounts of cells to cluster and break off from the tissue ring. Another possibility is inadequate trypsinizing/homogenization of cell suspension. If trypsinization is not adequately performed there may be small clusters of cells which naturally drift apart from the cell suspension to form their own aggregates. However, a lack of trypsinization being responsible for the spheroids seems less likely due to vigorous admixing of the cell suspension performed prior to seeding.

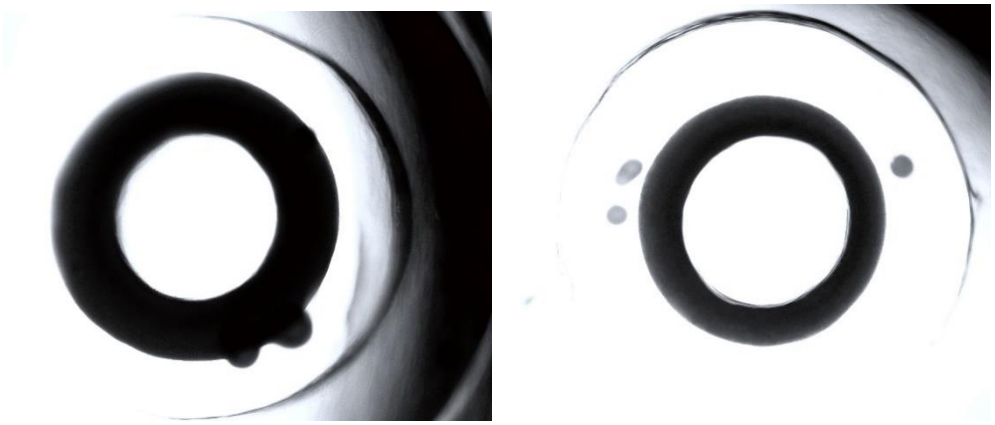

Figure 17: Representative images showing presence of cell spheroids taken at 2X magnification

The presence of the spheroids may have slightly affected the results as the spheroids were at times indiscernible from the rings themselves. The spheroids inconsistent position in the

agarose wells led to initial measurements sometimes including the spheroids in the total areas measured. However, once it became clear that these were independent entities, measurements were manually performed in ImageJ to exclude them from analysis.

Aim 2 focused on analyzing the structural and functional properties of NC and FT tissue rings via a histological and mechanical analysis.

Histology was performed to analyze the overall tissue morphology to determine if there was a difference in cellular alignment, density, or overall structure as a result of using freshly thawed cells. H&E was used to qualify these criteria, with no discernible differences being observed. To further analyze the structure and function of the cells, their ability to produce cell-derived extracellular matrix (ECM) in the form of collagen was analyzed using PRFG staining. The images from the PRFG staining also appeared similar, with both NC and FT tissue rings producing similar amounts of collagen with similar density and placement in the analyzed samples.

The last test performed for Aim 2 was uniaxial tensile testing. This test was used to evaluate the failure strain, UTS, and MTM of the tissue rings.

The collection of mechanical testing data proved to be the most challenging of all the tests performed due to software issues with the Instron preventing initial experiments from being run. Initial data were collected from experiments 3 and 4, however, these data were highly variable and experimental inconsistencies were observed from ring sample to ring sample. The sampling mounts for the Instron were initially causing the rings to lose their grip and fall off of the mounts once pre-cycling began. The faulty mounts caused some samples to experience more pre-cycling than others. Additionally, the rings had to be held down using a pair of forceps during pre-cycling to prevent any slippage, which may have affected the tissue ring's integrity. The raw data for these experiments can be seen in Appendix 8 however, the data were excluded from final analysis due to the noted inconsistencies and high variability, with moduli ranging from 9.02-4030 kPa. To address the initial issues in data collection, a new sampling mount was fashioned for experiment 6 (Appendix 9), however, the new sampling mount was not made of the same material as the predecessor and did not have its bending strength qualified, which could explain the discrepancy in mechanical properties found here compared to previous literature utilizing the tissue ring model.

The results stemming from mechanical testing were unexpected, as the FT tissue rings had higher values than the NC tissue rings across all 3 measurements, however the results were not statistically significant. The freshly thawed cell-derived rings having moderately higher values than their normally cultured counterpart could suggest that there is no difference in the mechanical properties measured, or that the spheroid formation previously mentioned, may have affected mechanical integrity.

Statistical post-hoc power analysis showed a distinct lack of power among 12/14 of the methods that were measured. However, the low powered results may not suggest a lack of significant findings. Post-Hoc power analysis is known to be misleading and in the case of non-inferiority testing a detriment to testing and analysis. Power in post-hoc analyses has been shown to be inversely proportional to the p-value, meaning that for high p-values, post-hoc analysis will return a low power.[50-51] Furthermore, the effect sizes obtained from the tests conducted in the final experiment suggest that to see sufficient power in all tests when using data obtained from the performed experiments we would need a minimum of 12,696 samples. For these two reasons, post-hoc analysis should not be relied upon to draw accurate sampling sizes and determine if sufficient power was reached. A priori sample size determination is generally the gold standard for ensuring sufficiently powered studies. Initial estimates were misinterpreted due to a misunderstanding within the G*Power software. When the correct values were input to determine the sample size, it again produced a total sample size that would be unrealistic to achieve (Table 3). The differences between the two groups may simply be attributed to sample-sample variation. Many tests had a larger %variance within each group than when the two groups were compared to each other. For example, strain data showed a higher average %variance within the NC tissue rings at 19.05%, whereas the %variance between the NC and FT groups was only 14.63%. These slight alterations in mechanical and structural properties, while not sufficiently powered, may not be biologically relevant. Furthermore, non-inferiority testing, or the “proving of the null hypothesis” often requires a much larger burden of proof and thus, significantly larger sample sizes when compared to looking for a statistical difference.[52]

Table 3: Corrected A Priori sample sizes depicting the total sample size required to achieve a power of 0.8 based on preliminary data of initial experiments

A priori (Power = 0.8)	Total sample size needed
AlamarBlue	76
UTS	58
Failure Strain	1018
MTM	48

Chapter 6: Conclusion & Future Work

6.1 Conclusion

Despite challenges encountered during testing, the collected data suggests that there is no overall loss in function or viability of tissues formed from freshly thawed (FT) cells compared to those that are cultured normally (NC) for several days before tissue formation. The only analysis showing a statistically significant lowered performance of FT rings was the 3-day alamarBlue measurement, which can either be explained as a difference in activity between FT and NC rings during the post-thaw recovery period, or interference by aggregated cells outside of the tissue ring constructs or outside the agarose wells on the well plate. While most tests found a lack of statistical significance, almost every test was found to be insufficiently powered, however, this may not be biologically significant, given the high amount of heterogeneity and variation within cell and tissue models. Thus, the data presented shows promise that under certain conditions, freshly thawed cells can be used just as effectively as normally cultured cells for tissue engineering applications.

6.2 Future Directions

There are several future directions that should be undertaken to quantify and qualify this body of research. The need to analyze varying cell types is one of the more important directions that can be further analyzed regarding the use of freshly thawed cells as a tissue engineering raw material. The rat aortic smooth muscle cells used for this study were unaffected by the change in conditions, which is a promising result, however, this lack of change may be due to the overall resilience of the cell line itself, where more sensitive cell lines or types of cells may have a more profound effect from their immediate use after being freshly thawed. Additionally, as the cells used in this thesis were a clonally expanded cell line, there was no risk of senescence or any issues that may result from the presence of Hayflick's limit. Thus, the investigation of freshly thawed primary cells as a raw material should be examined. Furthermore, primary cells have

more clinical and industrial relevance for tissue engineering applications and would thus provide more widely applicable data and results.

The use of alternative cell types also allows for further qualification of the freshly thawed cell method for tissue engineering. For instance, the study of human mesenchymal stem cells (hMSCs), could analyze the effects of freshly thawing these cells on their ability to differentiate into functional cell types (adipose, cartilage, bone, smooth muscle) or function in different, more widely researched ways than can be achieved with RASMCs. The next criterion that should be investigated is the maximal cell concentration that can be used to freeze cell banks and achieve engineered tissues from freshly thawed cells before a noticeable decrease in both initial cellular viability and functional tissue performance is observed. The use of a freshly thawed cell bank for tissue engineering has the potential to accelerate the tissue engineering workflow, however, this increase in efficiency becomes more apparent with higher freezing densities. Higher freezing densities allow for lower resource, time, and production costs, with larger numbers of cells being able to be sold, used, or frozen in a shorter amount of time. Additionally, many tissue manufacturing methods, such as 3D cell-only bioprinting, require vast numbers of cells to achieve successful results.

Finally, alternative tissue models should be investigated to see if these data remain consistent in other reproducible models, and ones that have significant differences. The model used for this experiment was a scaffold free, cell-only tissue model. The use of alternative methodology may give insight into the recovery and stability of using freshly thawed cells for tissue engineering. Additionally, the use of new models helps to understand the limits and applications of using freshly thawed cells.

References

1. Chang, D. K., Louis, M. R., Gimenez, A., & Reece, E. M. (2019). The basics of Integra dermal regeneration template and its expanding clinical applications. *Seminars in Plastic Surgery*, *33*(03), 185–189. https://doi.org/10.1055/s-0039-1693401
2. Ho, S. Y. M., Nallanthamby, V., & Wong, M. T. C. (2010). Accelerated Osteomesh Resorption: A case report. *Craniomaxillofacial Trauma & Reconstruction*, *3*(3), 115–117. https://doi.org/10.1055/s-0030-1254379
3. Seyhan, A. A. (2019). Lost in translation: The Valley of death across preclinical and clinical divide – identification of problems and overcoming obstacles. *Translational Medicine Communications*, *4*(1). https://doi.org/10.1186/s41231-019-0050-7
4. Husain, S. A., King, K. L., Pastan, S., Patzer, R. E., Cohen, D. J., Radhakrishnan, J., & Mohan, S. (2019). Association between declined offers of deceased donor kidney allograft and outcomes in kidney transplant candidates. *JAMA Network Open*, *2*(8). https://doi.org/10.1001/jamanetworkopen.2019.10312
5. Ikada, Y. (2006). Challenges in tissue engineering. *Royal Society Publishing* . https://doi.org/https://doi.org/10.1098/rsif.2006.0124
6. Miller, J. S. (2014). The billion cell construct: Will three-dimensional printing get us there? *PLoS Biology*, *12*(6). https://doi.org/10.1371/journal.pbio.1001882
7. Kim, J.-H., Kawase, E., Bharti, K., Karnieli, O., Arakawa, Y., & Stacey, G. (2022). Perspectives on the cost of goods for hpsc banks for manufacture of cell therapies. *Npj Regenerative Medicine*, *7*(1). https://doi.org/10.1038/s41536-022-00242-7
8. Melero-Martin, J. M., Santhalingam, S., & Al-Rubeai, M. (2008). Methodology for optimal in vitro cell expansion in tissue engineering. *Advances in Biochemical Engineering/Biotechnology*. https://doi.org/10.1007/10_2008_12
9. Sun, T., Jackson, S., Haycock, J. W., & MacNeil, S. (2006). Culture of skin cells in 3D rather than 2D improves their ability to survive exposure to cytotoxic agents. *Journal of Biotechnology*, *122*(3), 372–381. https://doi.org/10.1016/j.jbiotec.2005.12.021
10. Baust, J. M., Campbell, L. H., & Harbell, J. W. (2017). Best practices for cryopreserving, thawing, recovering, and assessing cells. *In Vitro Cellular & Developmental Biology - Animal*, *53*(10), 855–871. https://doi.org/10.1007/s11626-017-0201-y
11. Gwyther, T. A., Hu, J. Z., Christakis, A. G., Skorinko, J. K., Shaw, S. M., Billiar, K. L., & Rolle, M. W. (2011). Engineered vascular tissue fabricated from aggregated smooth muscle cells. *Cells Tissues Organs*, *194*(1), 13–24. https://doi.org/10.1159/000322554

12. Dash, B. C., Levi, K., Schwan, J., Luo, J., Bartulos, O., Wu, H., Qiu, C., Yi, T., Ren, Y., Campbell, S., Rolle, M. W., & Qyang, Y. (2016). Tissue-engineered vascular rings from human IPSC-derived smooth muscle cells. *Stem Cell Reports*, *7*(1), 19–28. https://doi.org/10.1016/j.stemcr.2016.05.004
13. Gwyther, T. A., Hu, J. Z., Billiar, K. L., & Rolle, M. W. (2011). Directed cellular self-assembly to fabricate cell-derived tissue rings for biomechanical analysis and Tissue Engineering. *Journal of Visualized Experiments*, (57). https://doi.org/10.3791/3366-v
14. Dikina, A. D., Alt, D. S., Herberg, S., McMillan, A., Strobel, H. A., Zheng, Z., Cao, M., Lai, B. P., Jeon, O., Petsinger, V. I., Cotton, C. U., Rolle, M. W., & Alsberg, E. (2018). A modular strategy to engineer complex tissues and organs. *Advanced Science*, *5*(5), 1700402. https://doi.org/10.1002/advs.201700402
15. Marzi, J., Brauchle, E. M., Schenke-Layland, K., & Rolle, M. W. (2019). Non-invasive functional molecular phenotyping of human smooth muscle cells utilized in cardiovascular tissue engineering. *Acta Biomaterialia*, *89*, 193–205. https://doi.org/10.1016/j.actbio.2019.03.026
16. Luo, J., Qin, L., Kural, M. H., Schwan, J., Li, X., Bartulos, O., Cong, X.-qiang, Ren, Y., Gui, L., Li, G., Ellis, M. W., Li, P., Kotton, D. N., Dardik, A., Pober, J. S., Tellides, G., Rolle, M., Campbell, S., Hawley, R. J., … Qyang, Y. (2017). Vascular smooth muscle cells derived from inbred swine induced pluripotent stem cells for vascular tissue engineering. *Biomaterials*, *147*, 116–132. https://doi.org/10.1016/j.biomaterials.2017.09.019
17. Adebayo, O., Hookway, T. A., Hu, J. Z., Billiar, K. L., & Rolle, M. W. (2012). Self-assembled smooth muscle cell tissue rings exhibit greater tensile strength than cell-seeded fibrin or Collagen Gel Rings. *Journal of Biomedical Materials Research Part A*, *101A*(2), 428–437. https://doi.org/10.1002/jbm.a.34341
18. Strobel, H. A., Dikina, A. D., Levi, K., Solorio, L. D., Alsberg, E., & Rolle, M. W. (2017). Cellular self-assembly with microsphere incorporation for growth factor delivery within engineered vascular tissue rings. *Tissue Engineering Part A*, *23*(3-4), 143–155. https://doi.org/10.1089/ten.tea.2016.0260
19. Strobel, H. A., Hookway, T. A., Piola, M., Fiore, G. B., Soncini, M., Alsberg, E., & Rolle, M. W. (2018). Assembly of tissue-engineered blood vessels with spatially controlled heterogeneities. *Tissue Engineering Part A*, *24*(19-20), 1492–1503. https://doi.org/10.1089/ten.tea.2017.0492
20. Strobel, H. A., Calamari, E. L., Alphonse, B., Hookway, T. A., & Rolle, M. W. (2018). Fabrication of custom agarose wells for cell seeding and Tissue Ring self-assembly using 3D-printed molds. *Journal of Visualized Experiments*, (134). https://doi.org/10.3791/56618
21. O'Brien, F. J. (2011). Biomaterials & scaffolds for tissue engineering. *Materials Today*, *14*(3), 88–95. https://doi.org/https://doi.org/10.1016/S1369-7021(11)70058-X.
22. Naderi, H., Matin, M. M., & Bahrami, A. R. (2011). Review paper: Critical issues in tissue engineering: Biomaterials, cell sources, angiogenesis, and Drug Delivery Systems. *Journal of Biomaterials Applications*, *26*(4), 383–417. https://doi.org/10.1177/0885328211408946
23. Madorran, E., Stožer, A., Bevc, S., & Maver, U. (2019). In vitro toxicity model: Upgrades to bridge the gap between preclinical and clinical research. *Bosnian Journal of Basic Medical Sciences*. https://doi.org/10.17305/bjbms.2019.4378

24. Marei, I., Abu Samaan, T., Al-Quradaghi, M. A., Farah, A. A., Mahmud, S. H., Ding, H., & Triggle, C. R. (2022). 3D tissue-engineered vascular drug screening platforms: Promise and considerations. *Frontiers in Cardiovascular Medicine*, *9*. https://doi.org/10.3389/fcvm.2022.847554
25. Duval, K., Grover, H., Han, L.-H., Mou, Y., Pegoraro, A. F., Fredberg, J., & Chen, Z. (2017). Modeling physiological events in 2D vs. 3D cell culture. *Physiology*, *32*(4), 266–277. https://doi.org/10.1152/physiol.00036.2016
26. Seyhan, A. A. (2019). Lost in translation: The Valley of death across preclinical and clinical divide – identification of problems and overcoming obstacles. *Translational Medicine Communications*, *4*(1). https://doi.org/10.1186/s41231-019-0050-7
27. Chan, B. P., & Leong, K. W. (2008). Scaffolding in tissue engineering: General approaches and tissue-specific considerations. *European Spine Journal*, *17*(S4), 467–479. https://doi.org/10.1007/s00586-008-0745-3
28. De Pieri, A., Rochev, Y., & Zeugolis, D. I. (2021). Scaffold-free cell-based tissue engineering therapies: Advances, shortfalls and forecast. *Npj Regenerative Medicine*, *6*(1). https://doi.org/10.1038/s41536-021-00133-3
29. DuRaine, G. D., Brown, W. E., Hu, J. C., & Athanasiou, K. A. (2014). Emergence of scaffold-free approaches for tissue engineering musculoskeletal cartilages. *Annals of Biomedical Engineering*, *43*(3), 543–554. https://doi.org/10.1007/s10439-014-1161-y
30. Assunção, M., Dehghan-Baniani, D., Yiu, C. H., Später, T., Beyer, S., & Blocki, A. (2020). Cell-derived extracellular matrix for tissue engineering and Regenerative Medicine. *Frontiers in Bioengineering and Biotechnology*, *8*. *https://doi.org/10.3389/fbioe.2020.602009*
31. Kumar, A., & Starly, B. (2015). Large scale industrialized cell expansion: Producing the critical raw material for Biofabrication Processes. *Biofabrication*, *7*(4), 044103. https://doi.org/10.1088/1758-5090/7/4/044103
32. Wrigley, J. D., McCall, E. J., Bannaghan, C. L., Liggins, L., Kendrick, C., Griffen, A., Hicks, R., & Fröderberg-Roth, L. (2014). Cell Banking for Pharmaceutical Research. *Drug Discovery Today*, *19*(10), 1518–1529. https://doi.org/10.1016/j.drudis.2014.05.006
33. Schiff, Leonard. J. (2005). Review: Production, characterization, and testing of banked mammalian cell substrates used to produce biological products. *In Vitro Cellular & Developmental Biology - Animal*, *41*(3), 65. https://doi.org/10.1290/0503024.1
34. Uhrig, M., Ezquer, F., & Ezquer, M. (2022). Improving cell recovery: Freezing and thawing optimization of induced pluripotent stem cells. *Cells*, *11*(5), 799. https://doi.org/10.3390/cells11050799
35. Matsumura, K., Rajan, R., & Ahmed, S. (2022). Bridging polymer chemistry and Cryobiology. *Polymer Journal*, *55*(2), 105–115. https://doi.org/10.1038/s41428-022-00735-8
36. Elliott, G. D., Wang, S., & Fuller, B. J. (2017). Cryoprotectants: A review of the actions and applications of cryoprotective solutes that modulate cell recovery from ultra-low temperatures. *Cryobiology*, *76*, 74–91. https://doi.org/10.1016/j.cryobiol.2017.04.004
37. Stacey, G. N., & Masters, J. R. (2008). Cryopreservation and banking of mammalian cell lines. *Nature Protocols*, *3*(12), 1981–1989. https://doi.org/10.1038/nprot.2008.190
38. Ben-David, U., Siranosian, B., Ha, G., Tang, H., Lyons, N. J., Burns, R., Nag, A., Cimini, B., Tsvetkov, P., Tubelli, A. A., Wong, B., Thorner, A. R., Bittker, J., Meyerson, M., Beroukhim, R., & Golub, T. R. (2018). Genetic and transcriptional instability alters cell

line drug response. Cancer Research, 78(560), 325–330. https://doi.org/10.1038/s41586-018-0409-3
39. Masters, J. R., & Stacey, G. N. (2007). Changing medium and passaging cell lines. Nature Protocols, 2(9), 2276–2284. https://doi.org/10.1038/nprot.2007.319
40. Quevedo, R., Smirnov, P., Tkachuk, D., Ho, C., El-Hachem, N., Safikhani, Z., Pugh, T. J., & Haibe-Kains, B. (2020). Assessment of genetic drift in large pharmacogenomic studies. Cell Systems, 11(4). https://doi.org/10.1016/j.cels.2020.08.012
41. Bojic, S., Murray, A., Bentley, B. L., Spindler, R., Pawlik, P., Cordeiro, J. L., Bauer, R., & de Magalhães, J. P. (2021). Winter is coming: The future of cryopreservation. *BMC Biology*, *19*(1). https://doi.org/10.1186/s12915-021-00976-8
42. Yokoyama, W. M., Thompson, M. L., & Ehrhardt, R. O. (2012). Cryopreservation and thawing of cells. *Current Protocols in Immunology*, *99*(1). https://doi.org/10.1002/0471142735.ima03gs99
43. Baust, J. G., Gao, D., & Baust, J. M. (2009). Cryopreservation. *Organogenesis*, *5*(3), 90–96. https://doi.org/10.4161/org.5.3.10021
44. Matsumura, K., Hayashi, F., Nagashima, T., Rajan, R., & Hyon, S.-H. (2021). Molecular mechanisms of cell cryopreservation with polyampholytes studied by solid-state NMR. *Communications Materials*, *2*(1). https://doi.org/10.1038/s43246-021-00118-1
45. Awan, M., Buriak, I., Fleck, R., Fuller, B., Goltsev, A., Kerby, J., Lowdell, M., Mericka, P., Petrenko, A., Petrenko, Y., Rogulska, O., Stolzing, A., & Stacey, G. N. (2020). Dimethyl sulfoxide: A central player since the dawn of Cryobiology, is efficacy balanced by toxicity? *Regenerative Medicine*, *15*(3), 1463–1491. https://doi.org/10.2217/rme-2019-0145
46. Sun, M., Liu, A., Yang, X., Gong, J., Yu, M., Yao, X., Wang, H., & He, Y. (2021). 3D cell culture—can it be as popular as 2D cell culture? *Advanced NanoBiomed Research*, *1*(5), 2000066. https://doi.org/10.1002/anbr.202000066
47. Lemire J., Covin C., White S., Giachelli C., Schwartz S. Characterization of cloned aortic smooth muscle cells from young rats. *Am J Pathol.* 1994;144:1068–1081.
48. Lemire J., Potter-Perigo S., Hall K., Wight T., Schwartz S. Distinct rat aortic smooth muscle cells differ in versican/PG-M expression. *Arterioscler Thromb Vasc Biol.* 1996;16:821–829.
49. Murray, K. A., & Gibson, M. I. (2022). Chemical approaches to cryopreservation. *Nature Reviews Chemistry*, *6*(8), 579–593. https://doi.org/10.1038/s41570-022-00407-4
50. Shreffler, J., & Huecker, M. R. (2023). Type I and Type II Errors and Statistical Power. *StatPearls*. Retrieved 2023, from https://www.ncbi.nlm.nih.gov/books/NBK557530/.
51. Kyonka, E. G. (2018). Tutorial: Small-N power analysis. *Perspectives on Behavior Science*, *42*(1), 133–152. https://doi.org/10.1007/s40614-018-0167-4
52. Streiner, D. L. (2003). Unicorns *do* exist: A tutorial on "proving" the null hypothesis. *The Canadian Journal of Psychiatry*, *48*(11), 756–761. https://doi.org/10.1177/070674370304801108

Appendices

Appendix 1: Outcomes measured across each experimental group with initial sample size noted (Performed indicates successful results whereas Not Performed indicates an error in testing which prevented the collection of data or performance of an assay)

	Outcomes Measured							
Experiment number	Initial Sample Size (NC)	Initial Sample Size (FT)	Initial Cell Viability	Structural Properties (area and thickness)	alamarBlue	Mechanical Testing	Live/Dead	Histology
Experiment 1	12	12	Performed	Not Performed	Performed	Not Performed	Performed	Performed
Experiment 2	12	12	Performed	Not Performed	Not Performed	Not Performed	Not Performed	Performed
Experiment 3	24	24	Performed	Performed	Not Performed	Not Performed	Performed	Performed
Experiment 4	12	12	Performed	Performed	Not Performed	Not Performed	Not Performed	Performed
Experiment 5	12	12	Performed	Not Performed	Performed	Performed	Performed	Not Performed
Experiment 6	24	24	Performed	Performed	Performed	Performed	Not Performed	Performed

Appendix 2: Examples of failed tissue ring samples. The sample on the left shows incomplete formation of a tissue ring that did not fully fuse to itself, and the sample on the right shows a sample with an incredibly thin region extremely prone to tearing

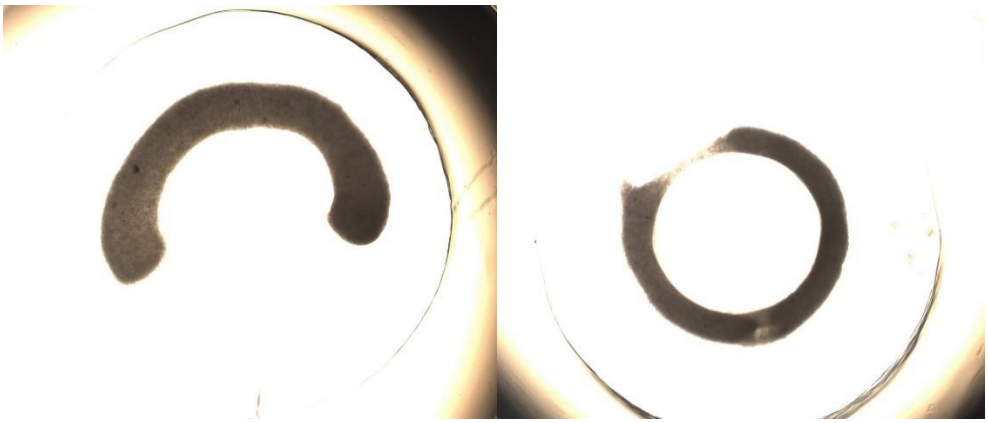

Appendix 3: Table plotting 7-day tissue ring development of 12 NC and 12 FT tissue rings

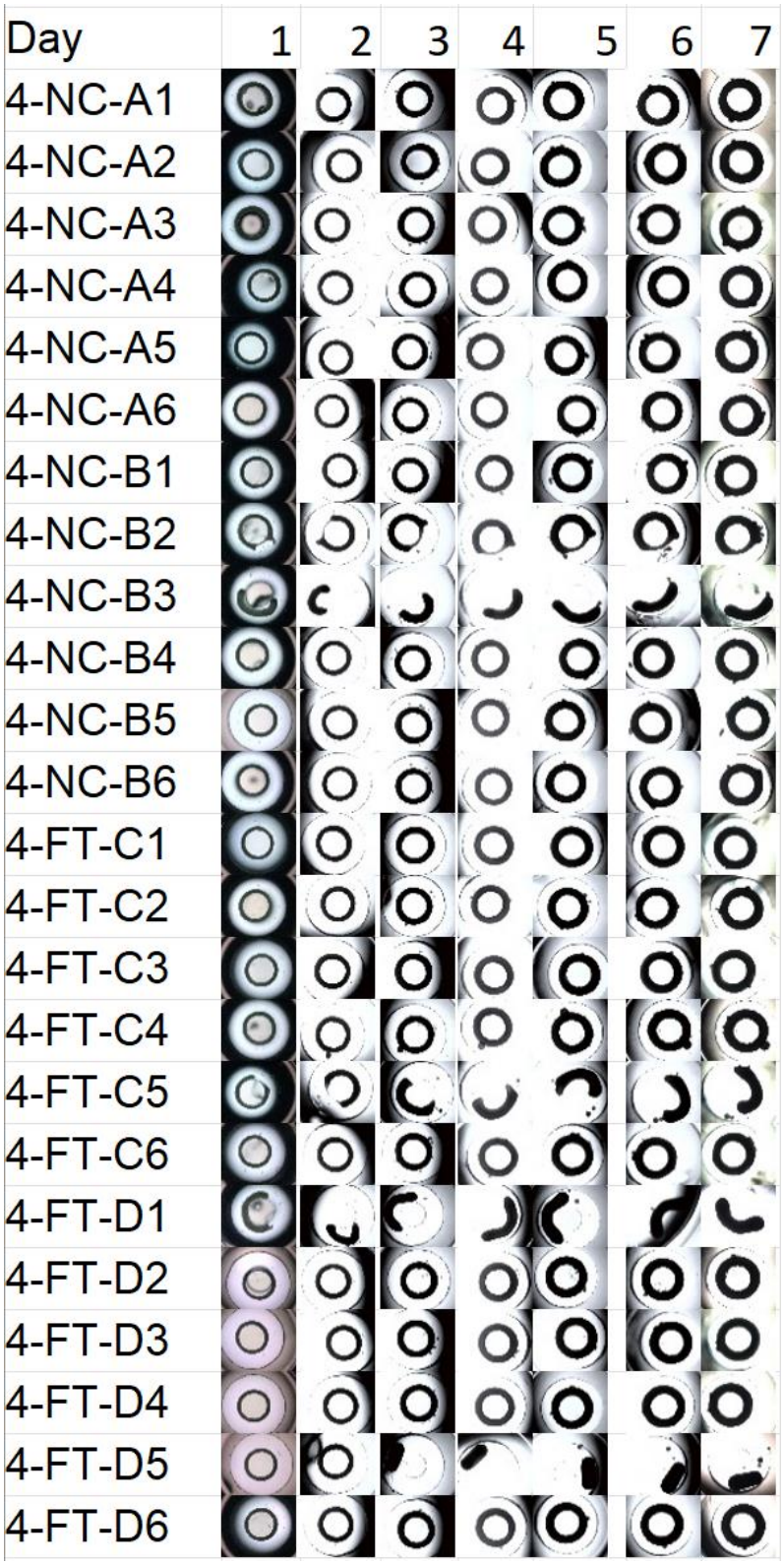

Appendix 4: Thickness dimensional data for all tested samples over 7 days (columns contain mean ± S.D.)

	NC Ring Sample Thickness (mm)	FT Ring Sample Thickness (mm)	NC sample size (n)	FT sample size (n)	p value
Day 1	0.357 ± 0.0340	0.332 ± 0.0310	23**	28**	0.0581
Day 2	0.425 ± 0.0550	0.410 ± 0.0520	46	46	0.7494
Day 3	0.499 ± 0.0600	0.496 ± 0.0510	45*	46	>0.9999
Day 4	0.571 ± 0.0800	0.567 ± 0.0770	45	46	>0.9999
Day 5	0.649 ± 0.0900	0.637 ± 0.0890	45	46	0.9949
Day 6	0.670 ± 0.0870	0.661 ± 0.0970	43*	45*	0.9995
Day 7	0.692 ± 0.0890	0.685 ± 0.111	45	44*	>0.9999

* Indicates tissue ring sample unable to be measured because of sample mishandling or image quality affecting ImageJ's ability to detect ring dimensions

** indicates loss of measurements due to data file corruption

Appendix 5: Average Metabolic activity across all alamarBlue testing measured in arbitrary absorbance units (rows contain mean ± S.D.)

	NC Absorbance (AU)	FT Absorbance (AU)	NC sample size(n)	FT sample size(n)	p value
Experiment 6 Day 3	370000 ± 160000	287000 ± 119000	21	21	0.0179
Experiment 6 Day 7	370000 ± 43100	395000 ± 57500	21	20	0.0595

Appendix 6: Average mechanical testing values found from UTS testing on Instron with outliers removed (rows contains the mean ± S.D.)

Sample	NC	FT
Average Failure Strain	2.88 ± 0.644	3.30 ± 0.609
Average UTS (KPa)	22.4 ± 5.09	30.2 ± 5.32
Average MTM (KPa)	7.98 ± 1.82	9.50 ± 1.51
n	11	15

Appendix 7: Half formed ring with artifact identified in agarose wells during tissue ring culture

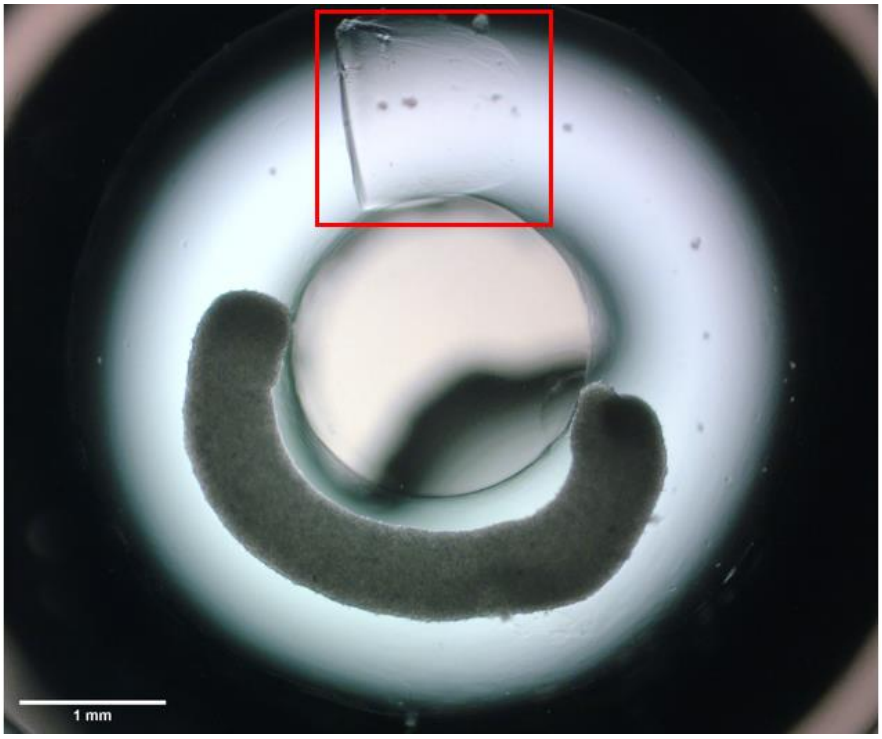

Appendix 8: Raw initial mechanical testing values found from UTS testing on Instron

Sample	Failure Strain	UTS (kPa)	MTM (kPa)
NC 1	0.256	17.5	68.5
NC 2	0.575	10.2	17.8
NC 3	1.19	16.7	14.1
NC 4	0.00580	23.3	4030
NC 5	1.65	17.1	10.3
NC 6	1.27	19.3	15.2
NC 7	1.48	18.7	12.7
FT 1	1.55	16.4	10.6
FT 2	1.75	13.7	7.84
FT 3	0.694	6.26	9.02
FT 4	1.28	15.2	11.9
FT 5	0.120	13.9	116
FT 6	0.833	16.3	19.5
FT 7	1.70	16.3	9.62

Appendix 9: Custom tissue sample pins (standard pictured above, and newly fashioned pin pictured below)